UNITED NATIONS EDUCATIONAL, SCIENTIFIC AND CULTURAL ORGANIZATION
INTERNATIONAL ATOMIC ENERGY AGENCY
INTERNATIONAL CENTRE FOR THEORETICAL PHYSICS
I.C.T.P., P.O. BOX 586, 34100 TRIESTE, ITALY, CABLE: CENTRATOM TRIESTE

SMR.961 - 5

WORKSHOP ON:
PROTEINS, MEMBRANES and their INTERACTIONS

22 JULY - 2 AUGUST 1996

"Modelling lipid membranes by diblock bilayers"

Michael SCHICK
University of Washington
Department of Physics Fm-15
Box 351560
WA 98195-1560 Seattle
U.S.A.

MODELLING LIPID MEMBRANES BY DIBLOCK BILAYERS

I. Diblock Polymorphism

II. Calculated Diblock Behavior (SCFT)

III. Addition of Homopolymer

IV. Rupture of a Bilayer

V. Pore Formation

   i Equilibrium Phase of Pores

   ii Formation of Pores by Fluctuations (Simulation)

VI. Bilayer of Semiflexible Diblock: Main Transition

A-B	Microstructure
PI-PS	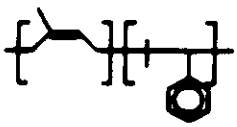
PE-PEE	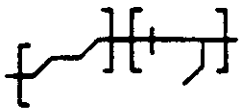
PEP-PEE	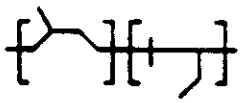
PE-PEP	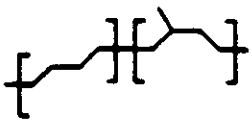

LAMELLAR PHASES

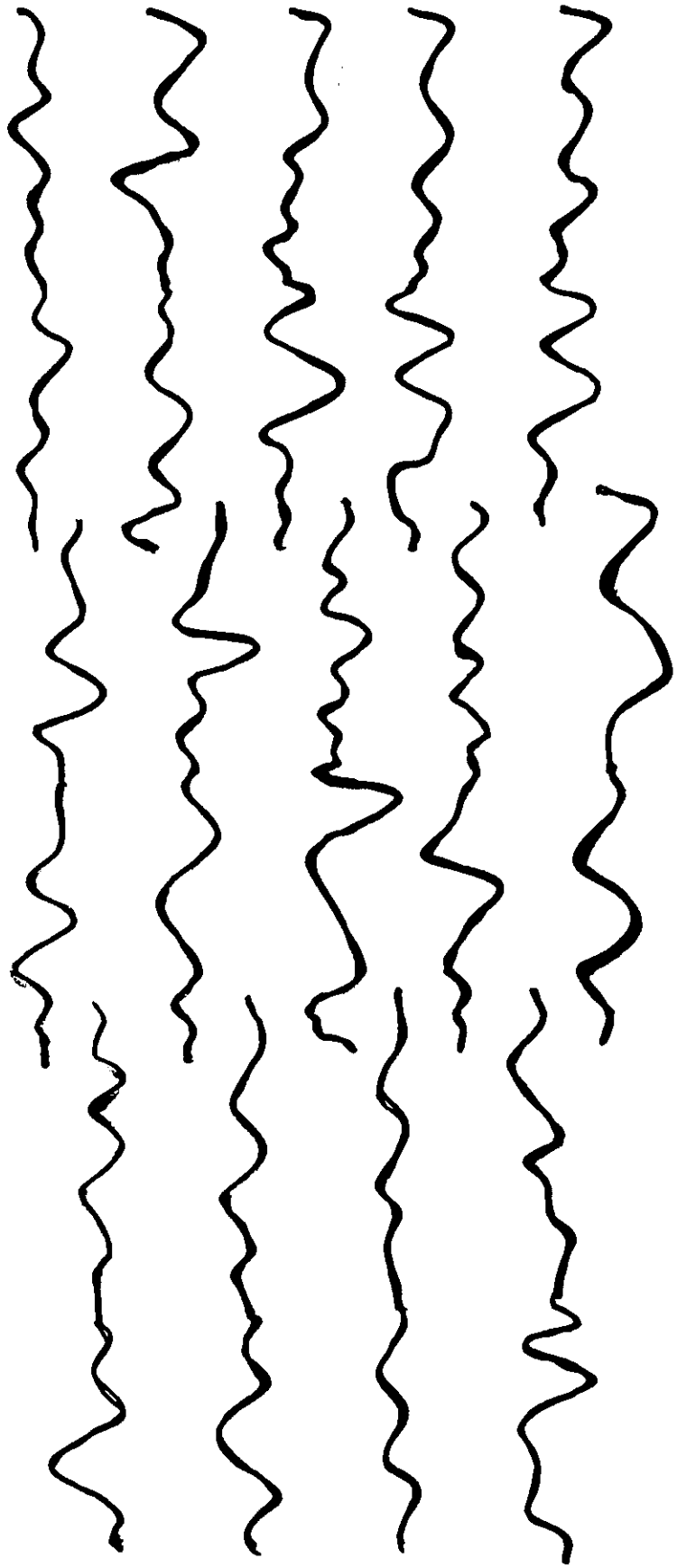

LAMELLAR PHASE OF POLYSTYRENE-POLYISOPRENE

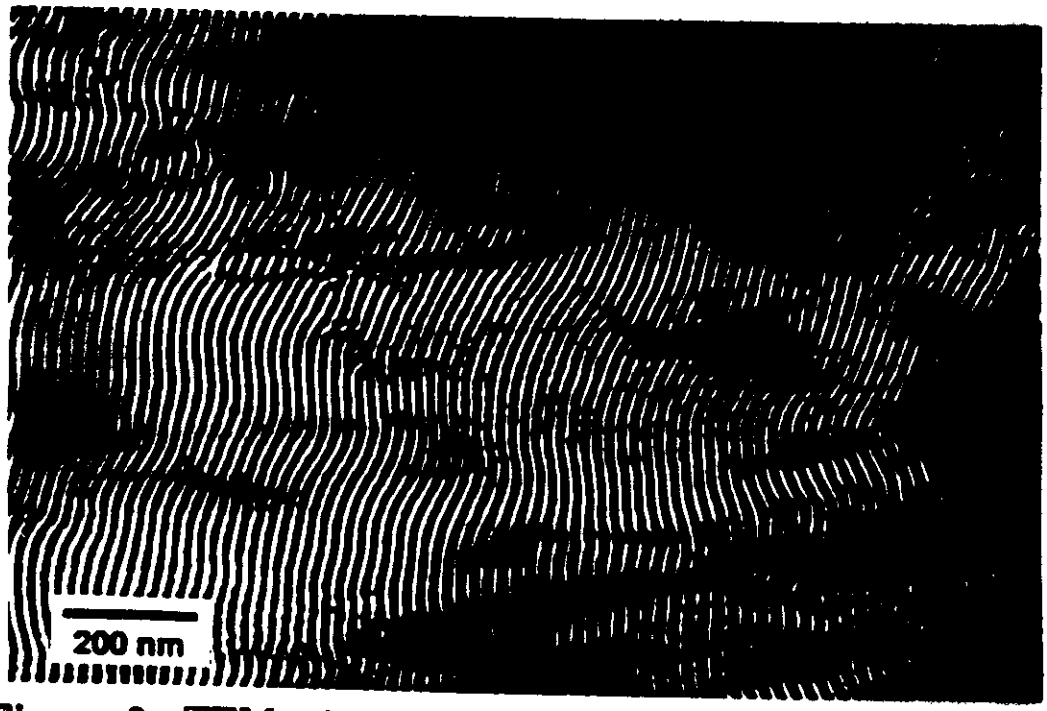

Figure 2. TEM micrograph of a sample of pure diblock cast from toluene and annealed for 1 week at 115 °C. Polyisoprene domains have been stained with OsO_4 to provide contrast and appear dark in the image. A well-ordered lamellar morphology with a repeat period of approximately 210 Å is clearly evident.

HADJUK ET AL. MACROMOLECULES 27, 4063 (1994)

OTHER PHASES

HEXAGONAL

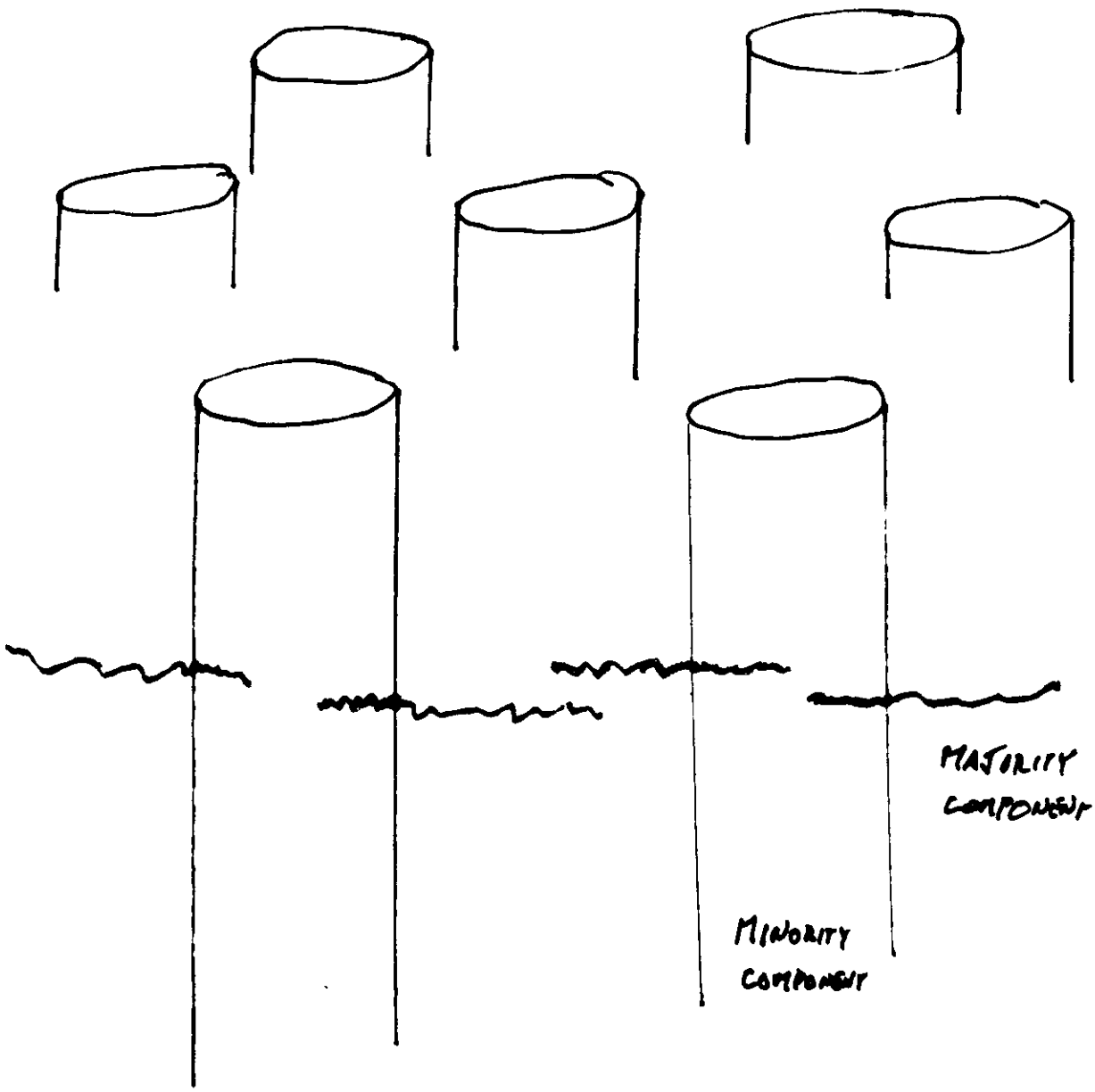

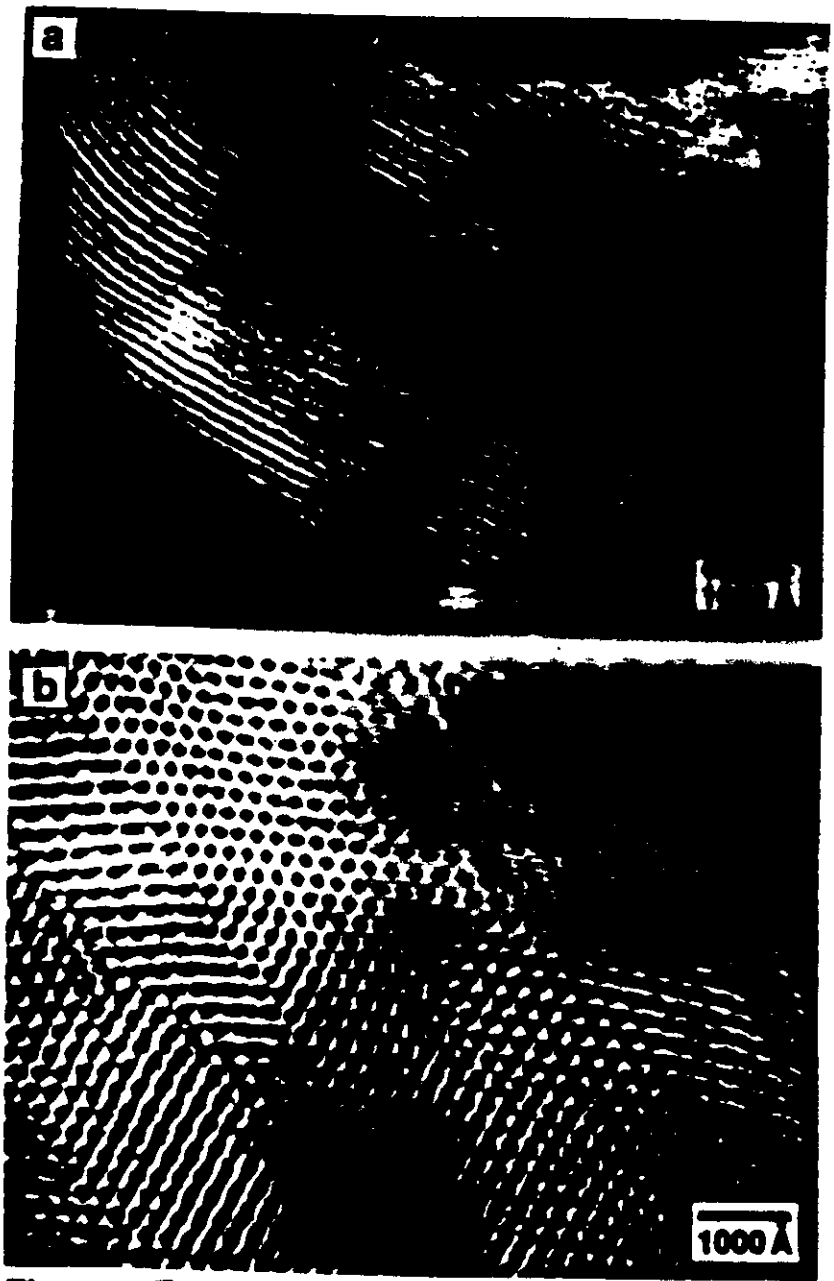

LAM

HEX

Figure 5. Transmission electron micrographs of (a) IS-42 in phase A (annealed at 145 °C) and (b) IS-33 in phase C (annealed at 145 °C), showing lamellar (LAM) and hexagonally packed cylinder (HEX) structures, respectively.

FÖRSTER ET AL. MACROMOLECULES 27, 6922 (1994)

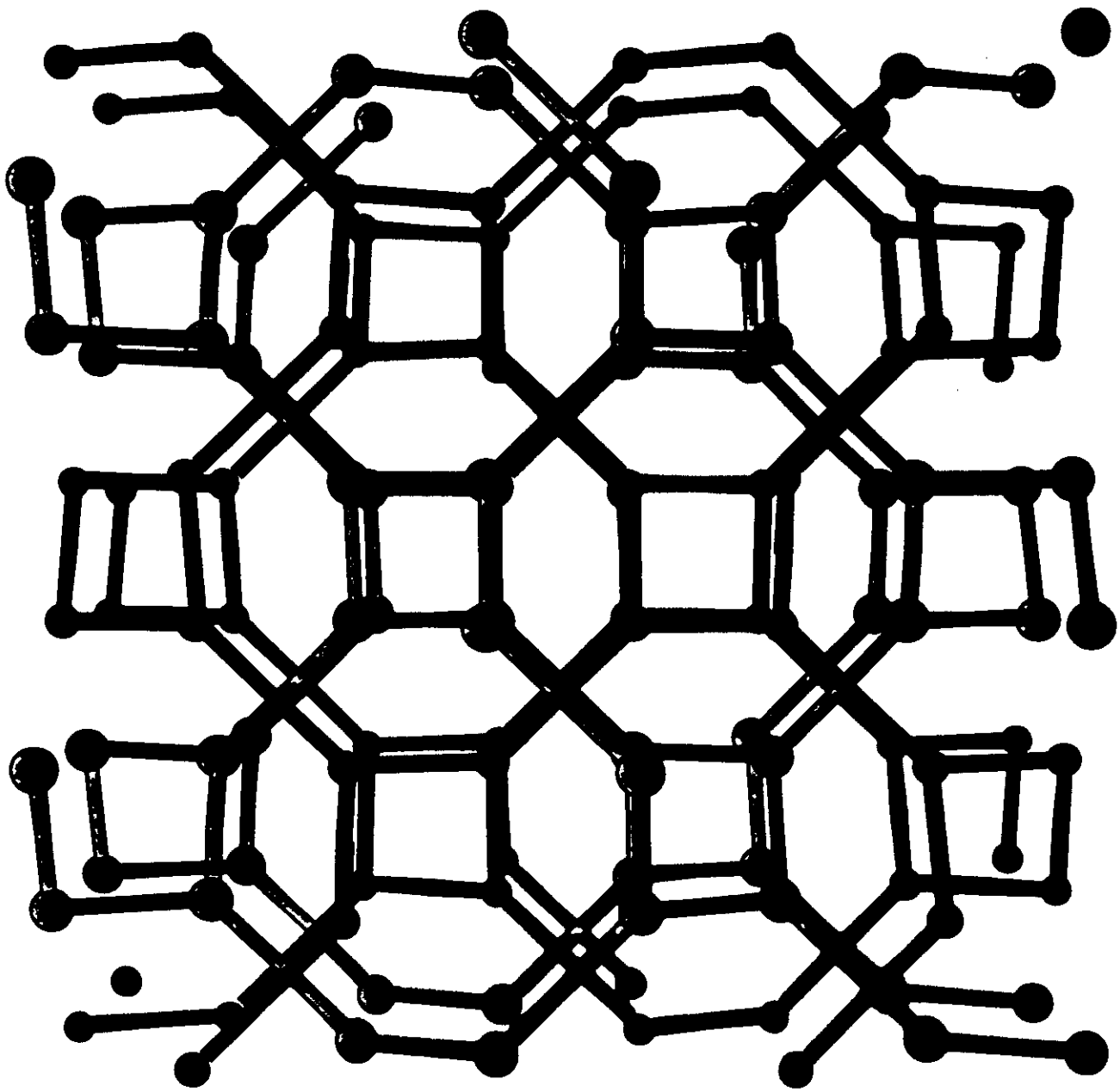

COURTESY OF A. FRANKEL

p

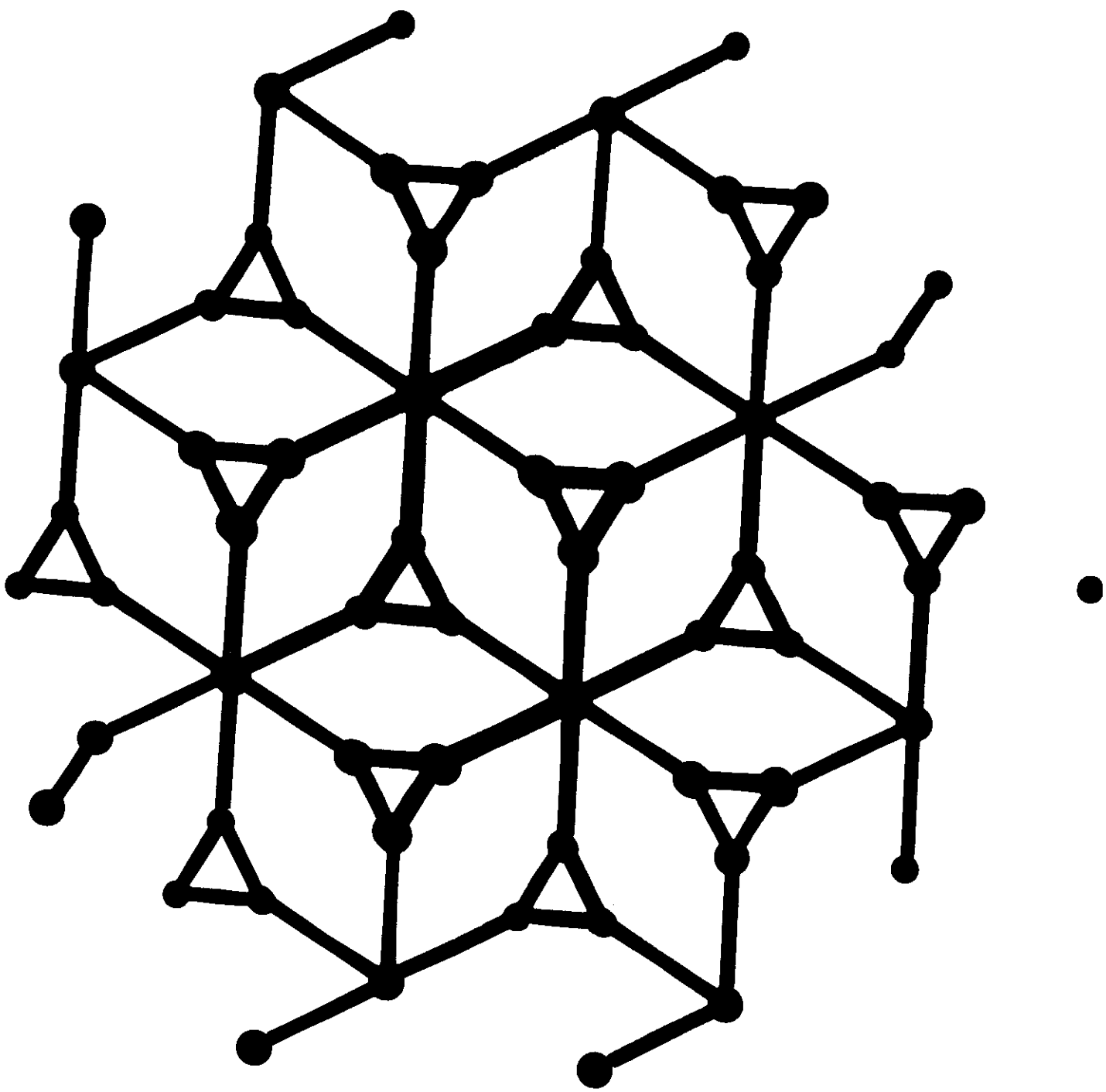

SAXS

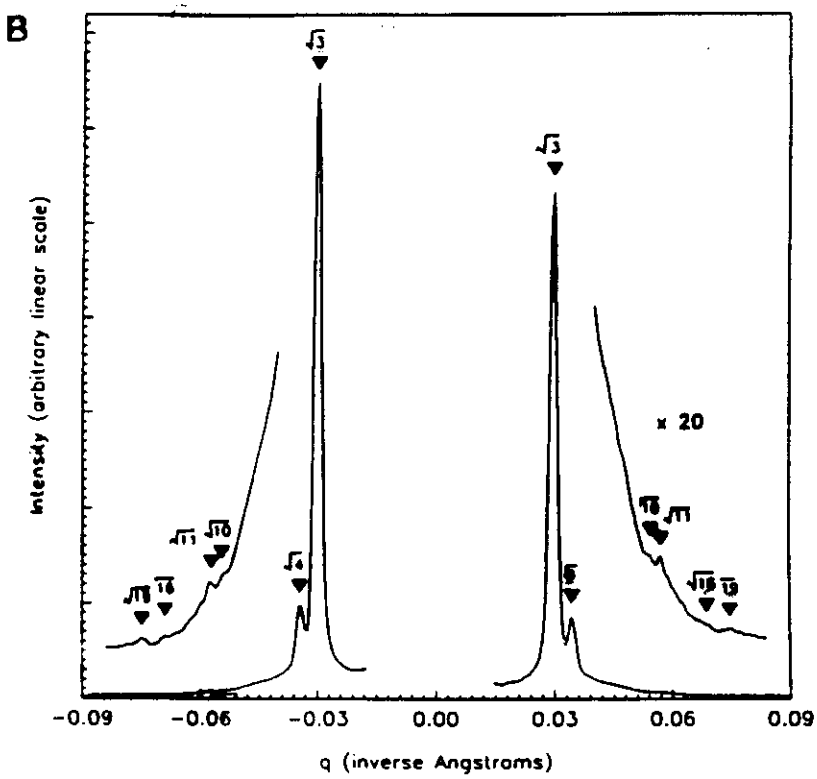

Figure 6. (A) Two-dimensional scattering image obtained from a pure diblock film annealed for 4 h at 150 °C to establish the new morphology, followed by quenching in liquid nitrogen and subsequent annealing at 120 °C for 4 h to eliminate disorder induced by quenching and increase the number of higher order Fourier components in the monomer concentration profile (as described in the text). This image was obtained after integrating for 8 h at 120 °C; comparison of diffraction before and after this period revealed no change in the scattering from the sample. (B) One-dimensional profile prepared from the two-dimensional image. $\sqrt{3}$, $\sqrt{4}$, $\sqrt{10}$, $\sqrt{11}$, $\sqrt{16}$, and $\sqrt{19}$ denote the position ratios of the observed reflections; as discussed in the text, such reflections are most consistent with a structure possessing *Ia*3*d* symmetry.

HAJDUK ET AL. MACROMOLECULES 27, 4063 (1994)

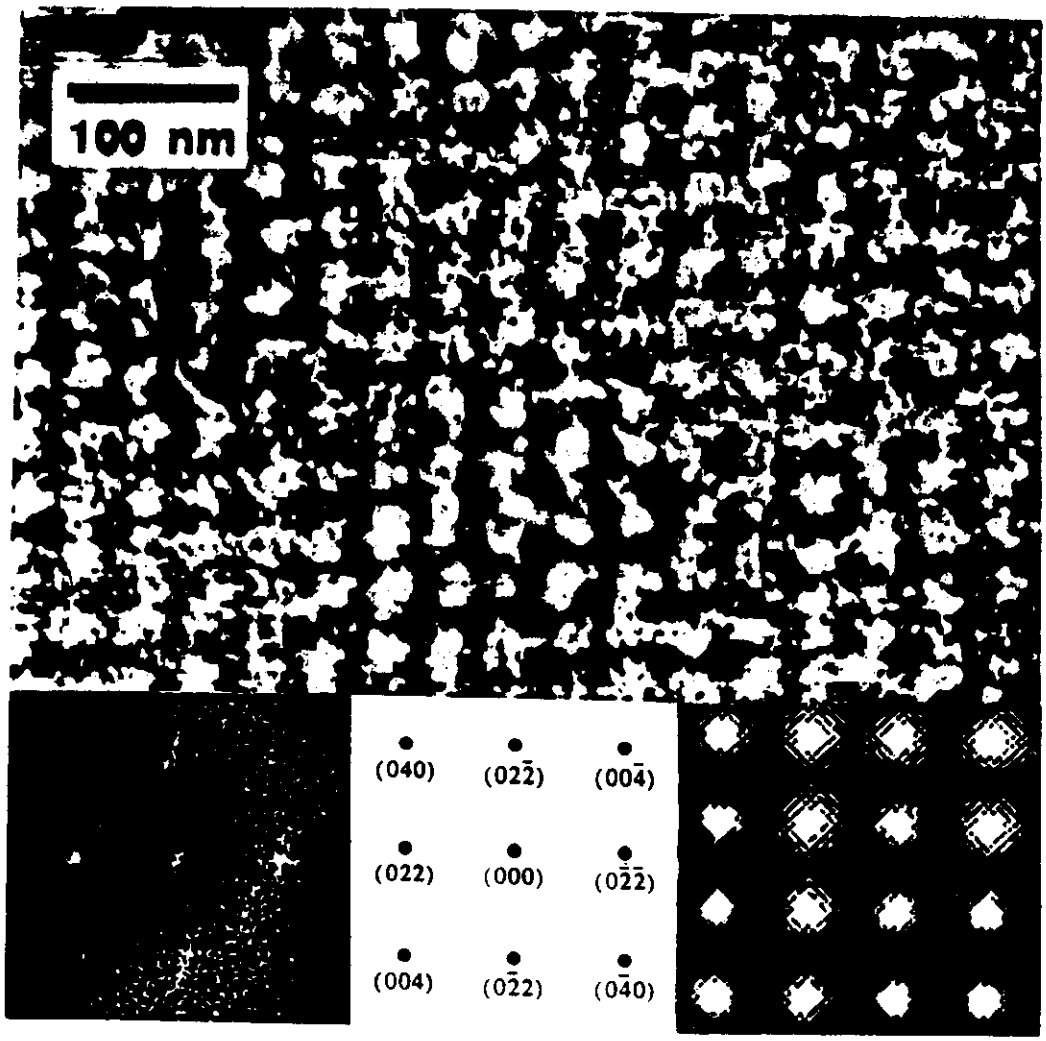

FIGURE 9

HADJUR ET AL. MACROMOLECULES 27, 4063 (1994)

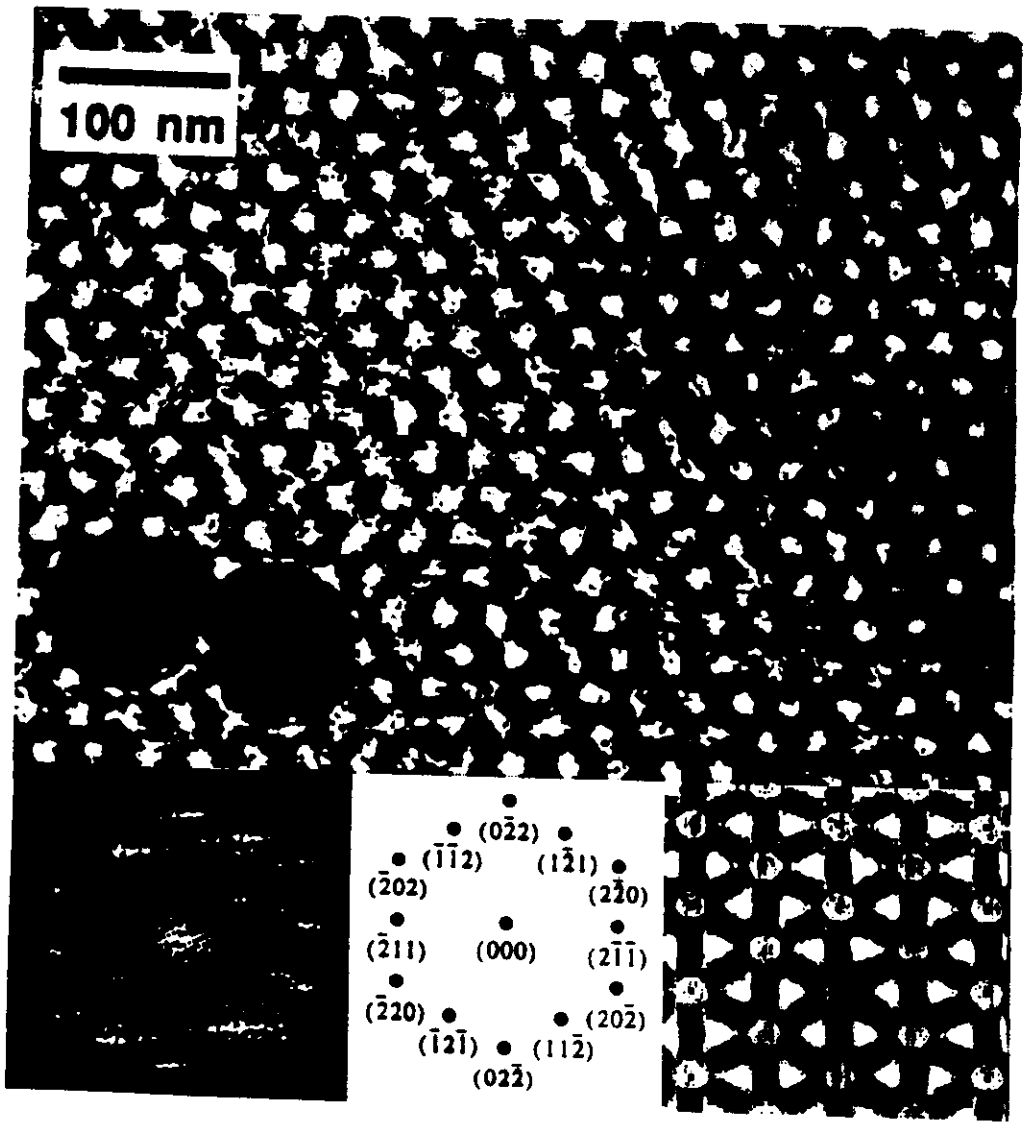

FIGURE 8

HAJDUK ET AL. MACROMOLECULES 27, 4063 (1994)

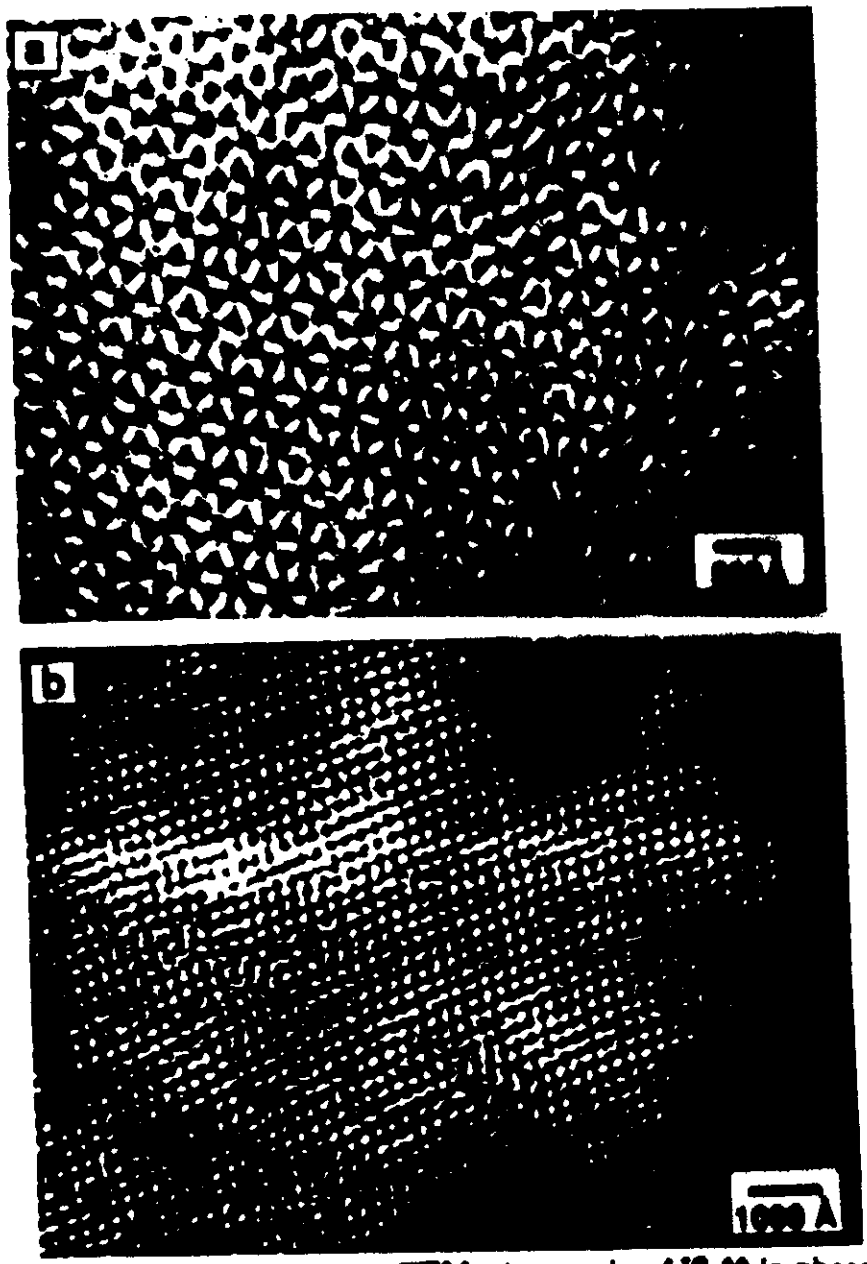

Figure 6. Representative TEM micrographs of IS-30 in phase B (annealed at 205 °C) showing (a) 3-fold and (b) 4-fold projections of the bicontinuous $Ia\bar{3}d$ microstructure.

FÖRSTER ET AL. MACROMOLECULES 27, 6922 (1994)

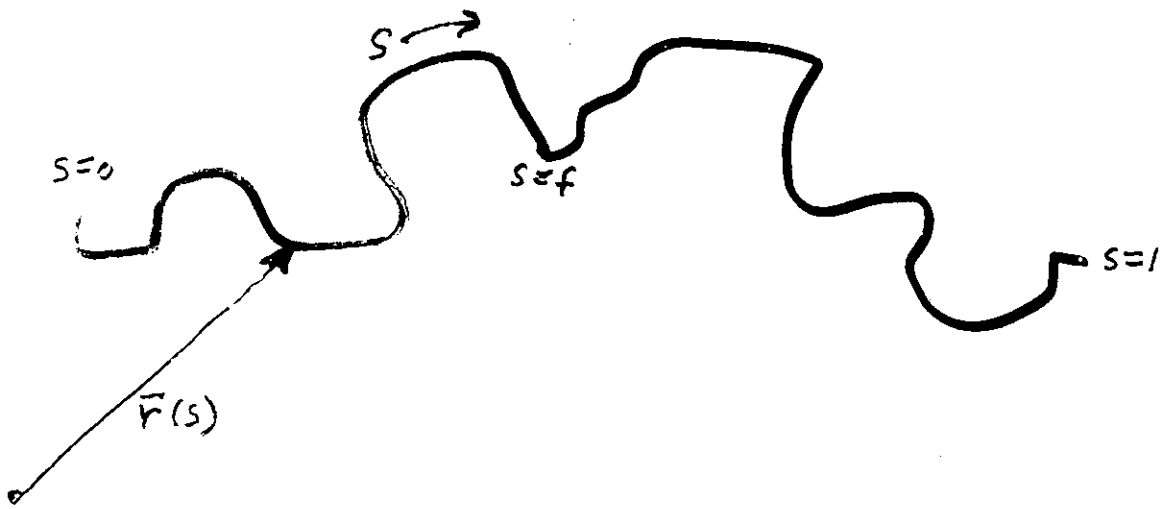

$$Q[w_A, w_B] \propto \int \mathcal{D}\mathbf{r} P[\mathbf{r}(s)] \exp - \left(\int_0^f ds w_A(\mathbf{r}(s)) + \int_f^1 ds w_B(\mathbf{r}(s)) \right)$$

where for flexible chains

$$P[\mathbf{r}(s)] = \exp\{-\frac{3}{2Na^2} \int_0^1 ds [\frac{d\mathbf{r}(s)}{ds}]^2\}$$

and for semi-flexible chains

$$P[\mathbf{r}(s)] = \exp\{-\frac{\kappa}{2N} \int_0^1 ds [\frac{d\mathbf{n}(s)}{ds}]^2\}$$

where

$$\mathbf{n}(s) \equiv \frac{1}{Na} \left(\frac{d\mathbf{r}(s)}{ds} \right)$$

INTERACTING POLYMER PROBLEM

Density of A monomers

$$\hat{\Phi}_A(\mathbf{r},\{\mathbf{r}(s)\}) = Nv\sum_{\alpha=1}^{n}\int_0^f ds\delta[\mathbf{r}-\mathbf{r}_\alpha(s)]$$

Density of B monomers

$$\hat{\Phi}_B(\mathbf{r},\{\mathbf{r}(s)\}) = Nv\sum_{\alpha=1}^{n}\int_f^1 ds\delta[\mathbf{r}-\mathbf{r}_\alpha(s)]$$

Interaction

$$+\chi\int\frac{d\mathbf{r}}{v}\hat{\Phi}_A(\mathbf{r})\hat{\Phi}_B(\mathbf{r})$$

Mean-Field Free Energy per Polymer

$$\frac{F_{mft}}{nkT} = -\ln Q[w_A,w_B] + \frac{1}{V}\int d\mathbf{r}\left(\frac{\chi N}{4}\left[\frac{w_A-w_B}{\chi N}-1\right]^2 - w_B\right)$$

where

$$w_A - w_B = \chi N(\phi_B-\phi_A)$$

$$\phi_A = <\hat{\Phi}_A> = -V\frac{\delta\ln Q[w_A,w_B]}{\delta w_A}$$

$$\phi_B = <\hat{\Phi}_B> = -V\frac{\delta\ln Q[w_A,w_B]}{\delta w_B}$$

$$1 = \phi_A+\phi_B$$

Expand all functions of position in complete set

of eigenfunctions of Laplacian

which have the desired space-group symmetry

$$w_A(\mathbf{r}) = \sum_i w_{Ai} f_i(\mathbf{r})$$

$$w_B(\mathbf{r}) = \sum_i w_{Bi} f_i(\mathbf{r})$$

.....

where

$$\nabla^2 f_i(\mathbf{r}) = \lambda_i D^{-2} f_i(\mathbf{r})$$

Matsen and Schick, PRL**72** 2660 (1994).

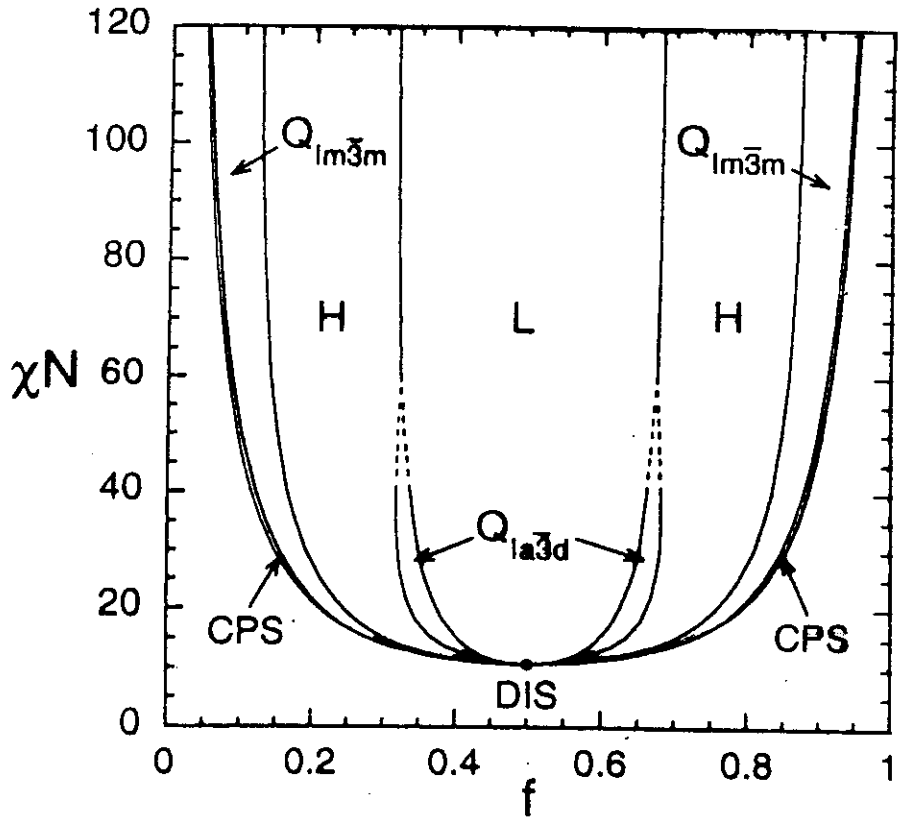

Figure 4, Matsen and Bates, Macromolecules (Review) 29, 1091 (1996)

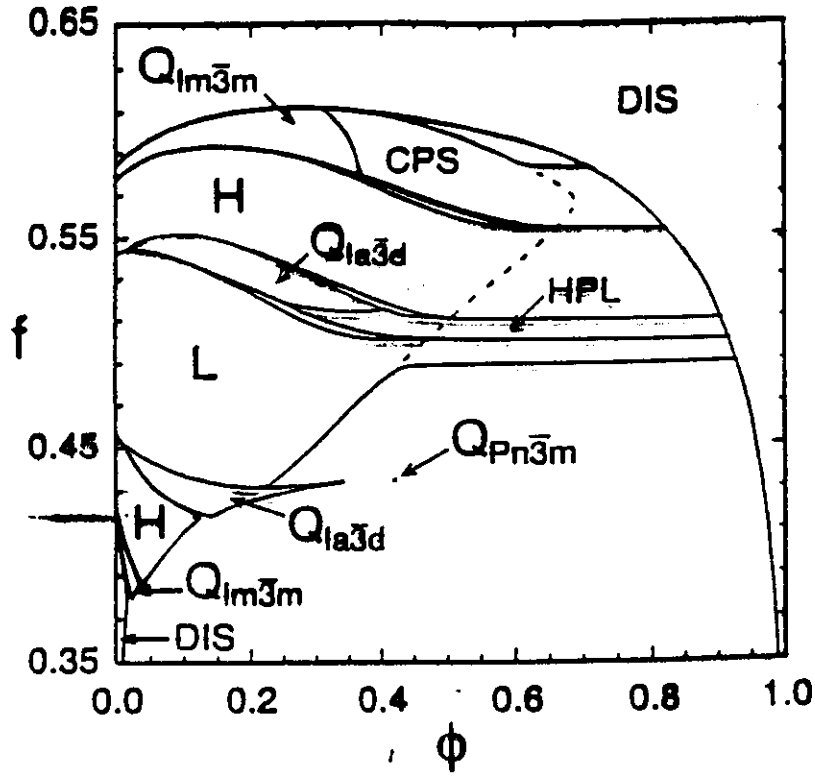

FIG. 1. **Phase** diagram for blends of AB diblock and A homopolymer at $\chi N = 11$ and equal polymerization indexes ($\alpha = 1$) plotted in terms of the homopolymer volume frac-

MATSEN, PRL 74, 4225 (1995)

NOW ADD SOLVENT (A HOMOPOLYMER)

TO AB DIBLOCK

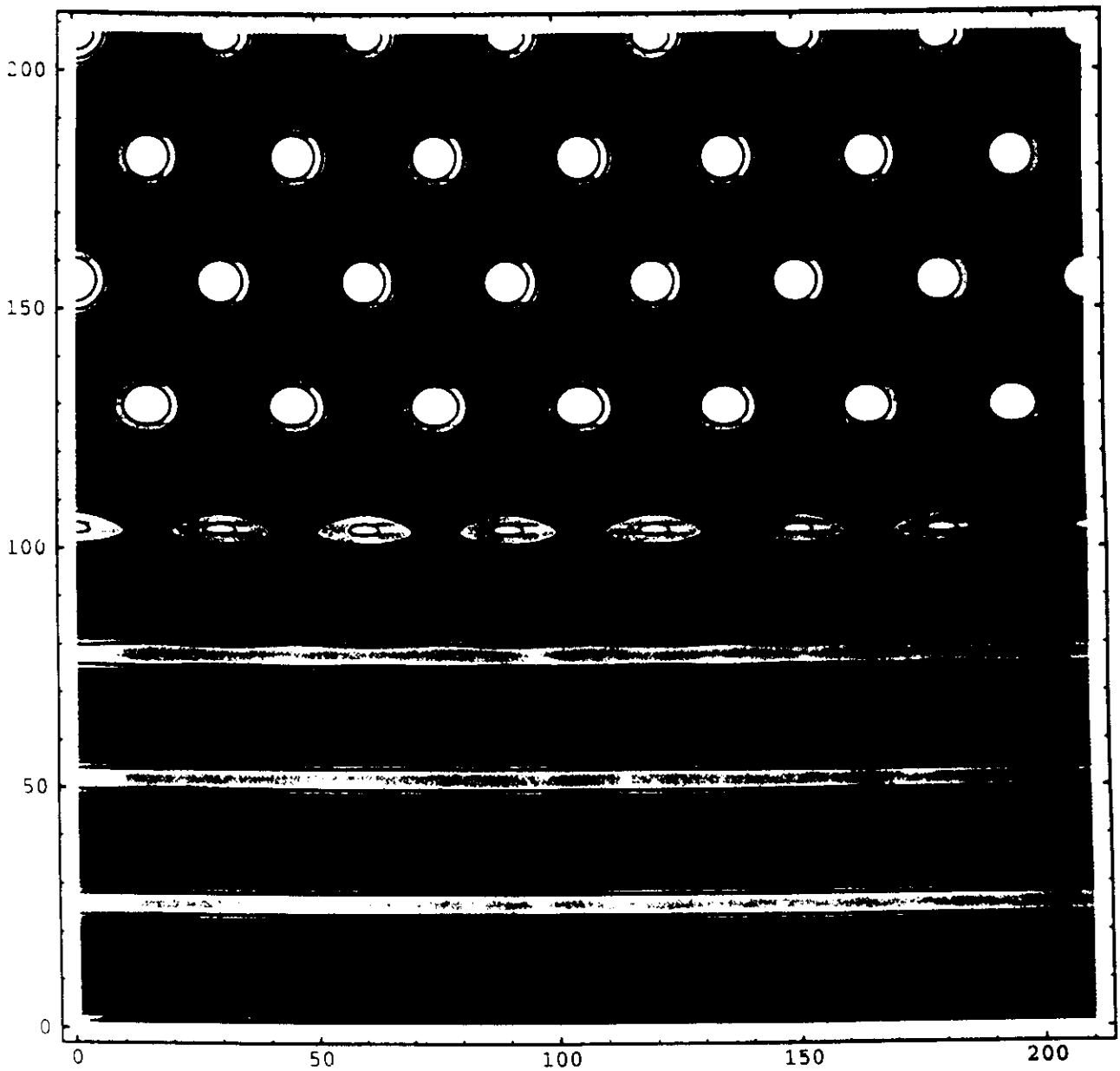
200
150
100
50
0
0
50
100
150
200

CATENOID LAMELLAR

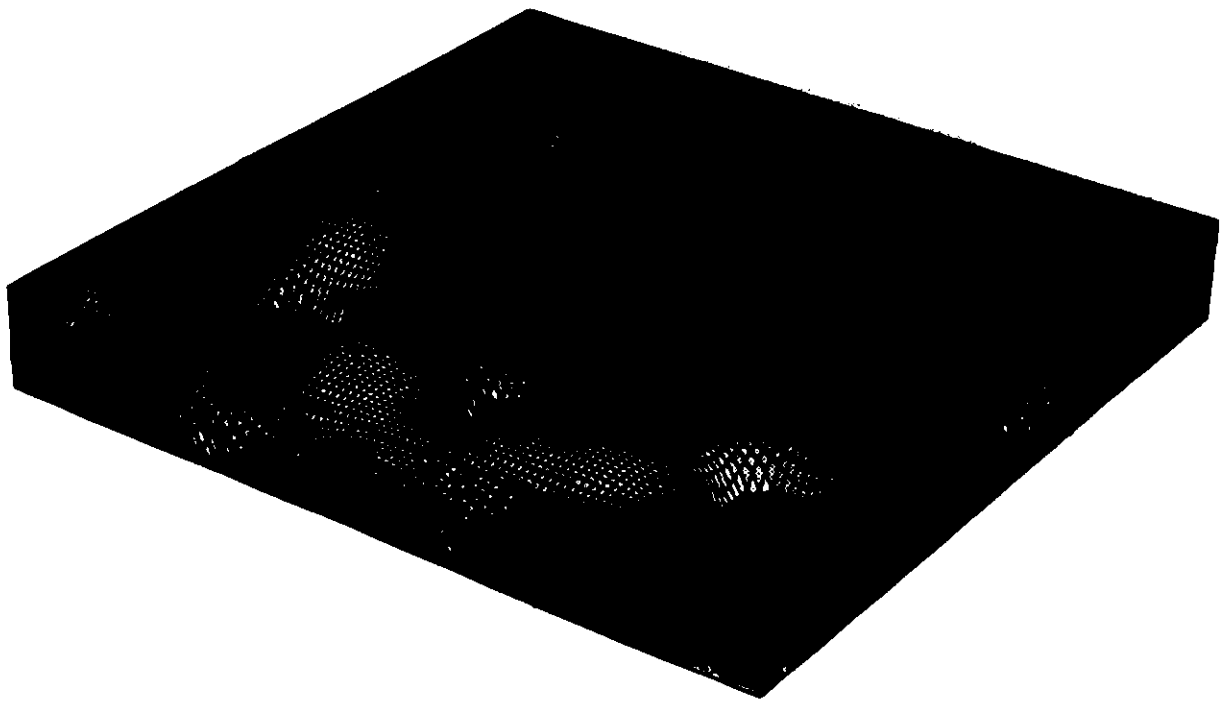

CATENOID LAMELLAR PHASE OBSERVED

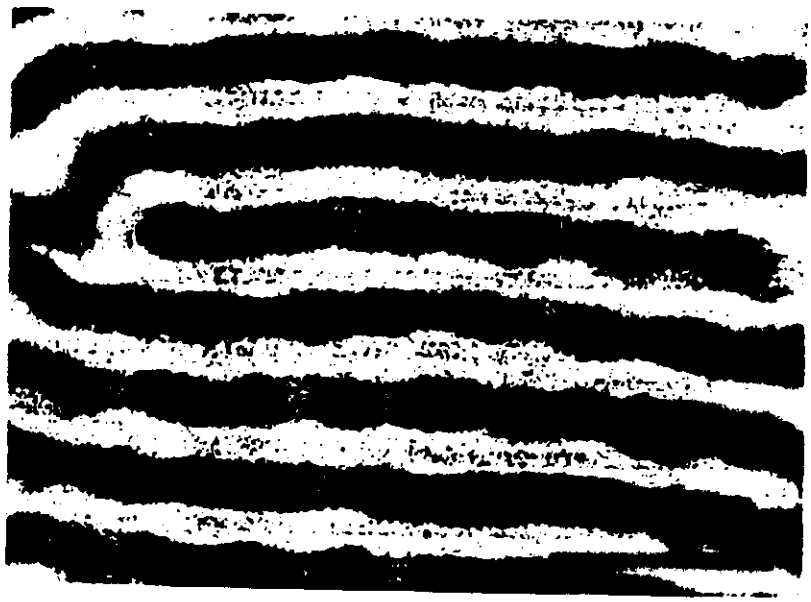

(a)

Figure 2. Transmission electron micrographs of an OsO_4-stained sample prepared from symmetric SB diblock for an edge-on view that is parallel to the lamellae (a) and a view norm to the layers (b). The shapes of punctured butadiene layers suggest a catenoidal shape for the butadiene layers. Scale markers are 100 nm.

STYRENE-BUTADIENE

DISKO ET AL. MACROMOLECULES 26, 2983 (1993)

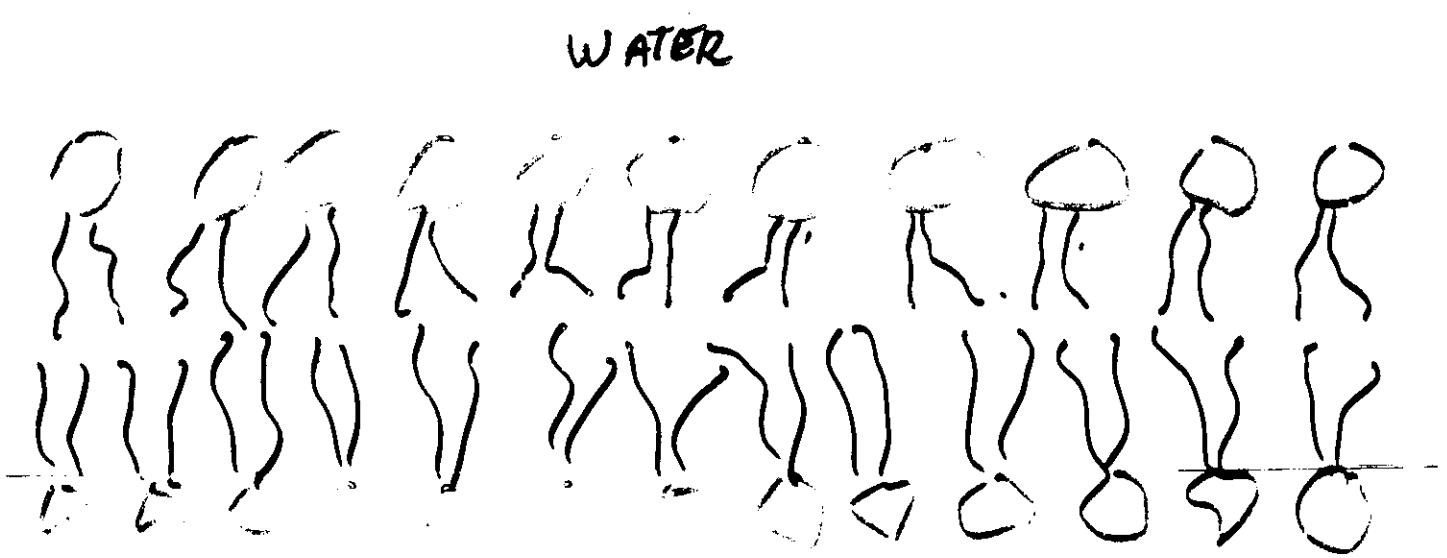
WATER

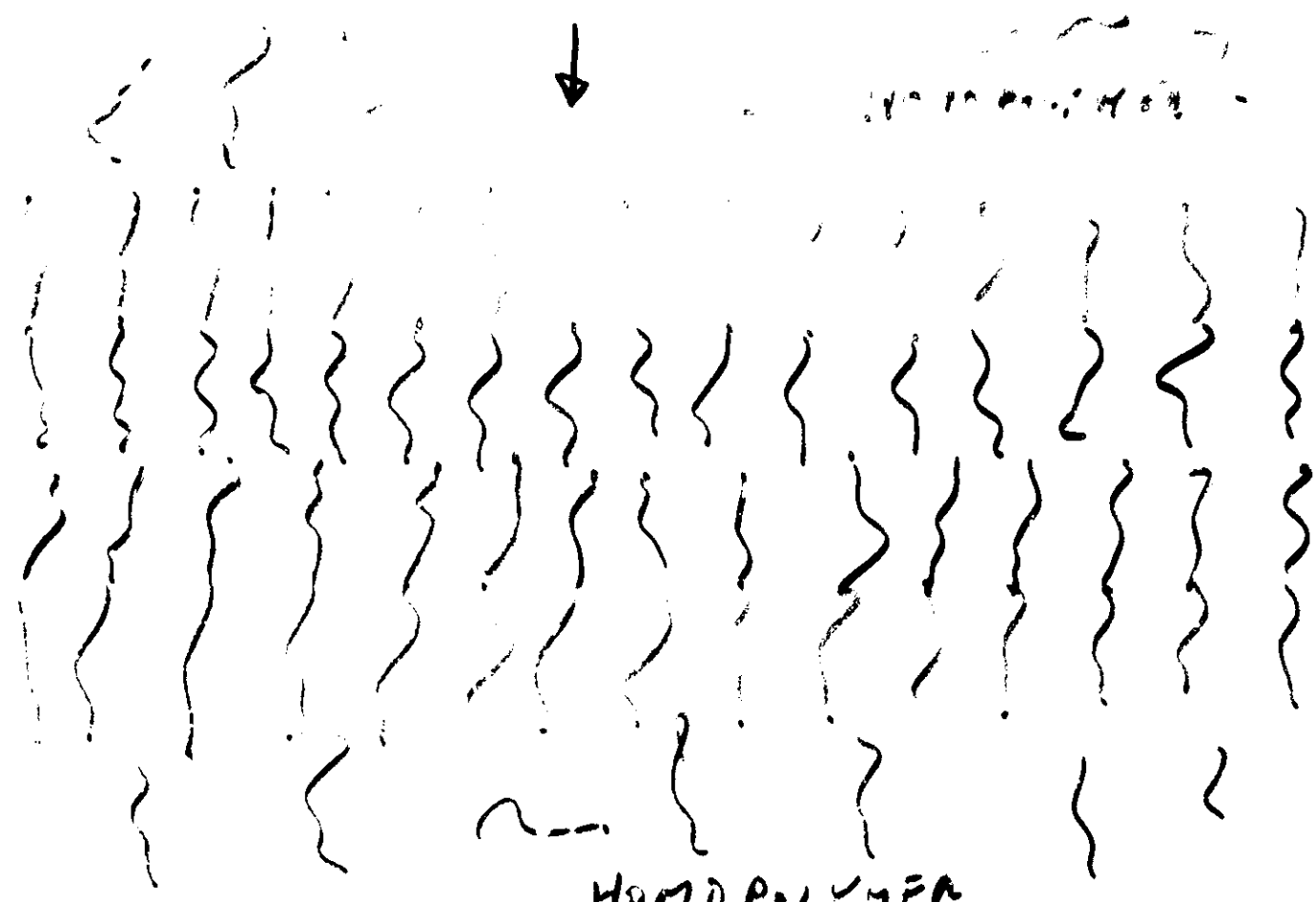
WATER
HOMOPOLYMER

embrane rupture—vesicle aspiration techniques

E. Evans

surface tension

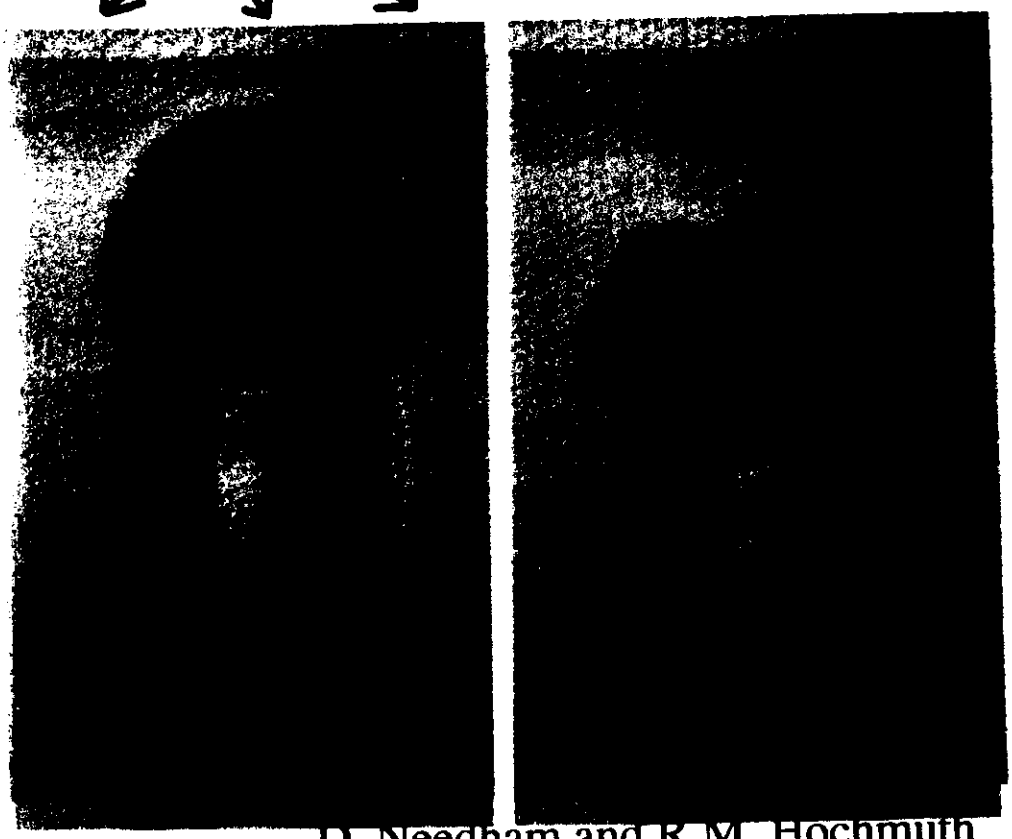

electric field pulse

tion
ssure

B. Needham and R.M. Hochmuth
B. Needham and R.M. Hochmuth
Biophysical Journal, 1989
Biophysical Journal, 1989

area extension at rupture: 2%-5%

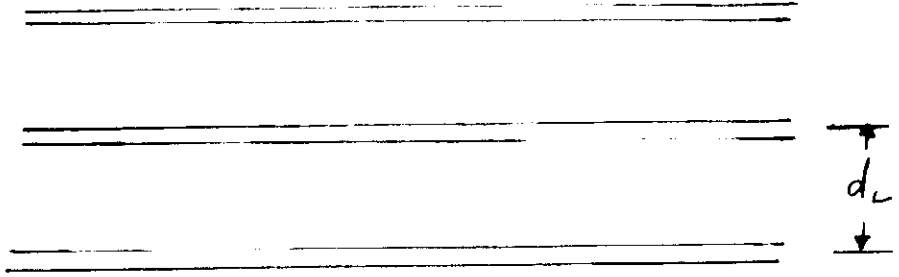

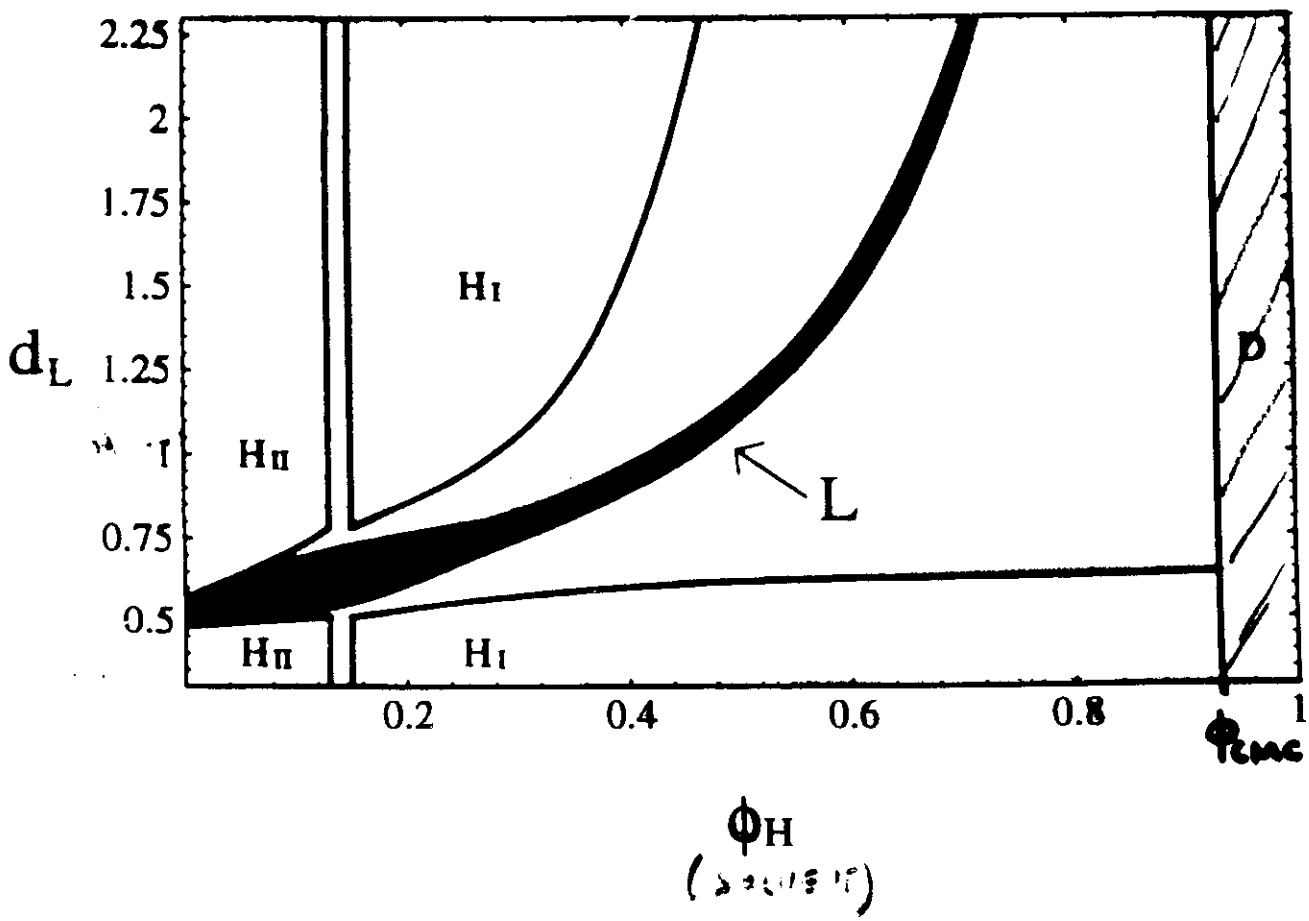

$f \approx 0.49$ (BULKY TAILS)

D. WEEZ & M. SCHICK, PRE 53, 3875 (1996)

Netz and Schick, Fig.4

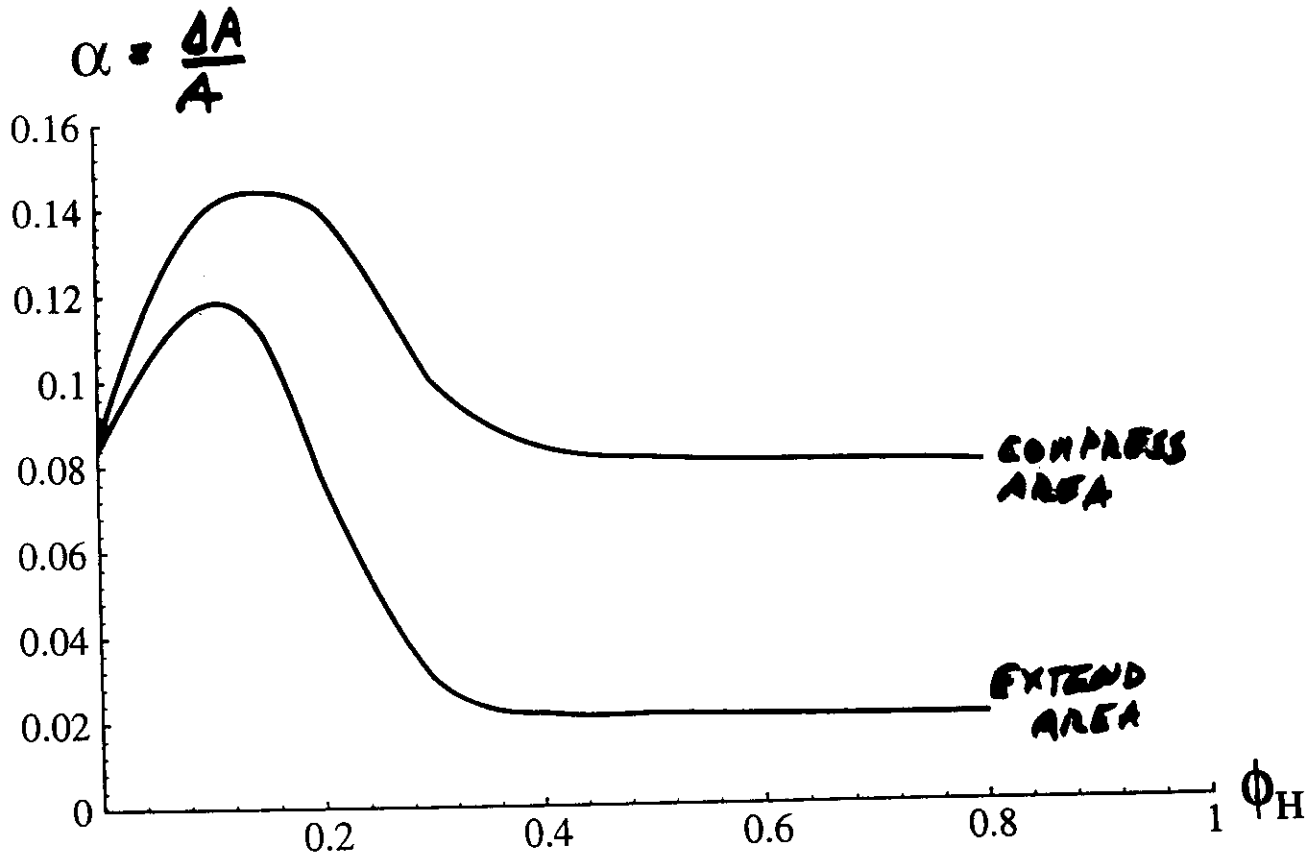

Formation of Pores

D.C. Chang, 1992

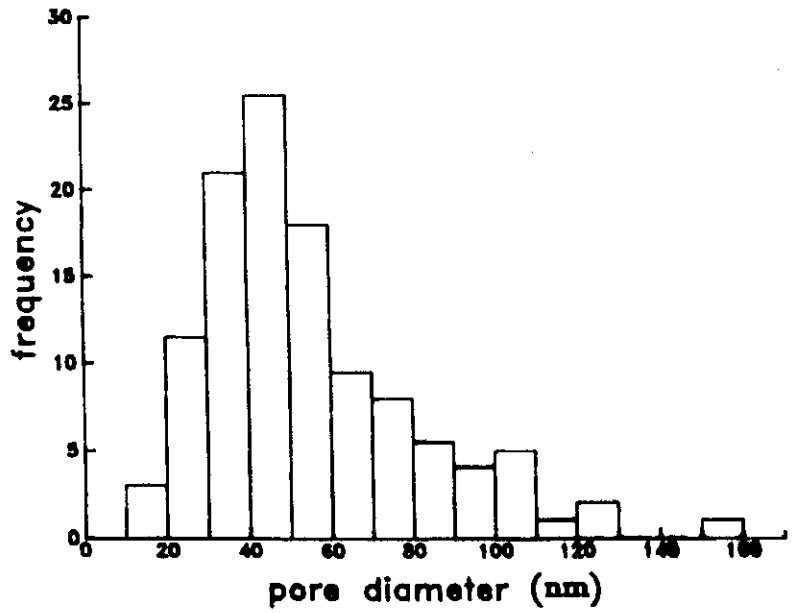

Guide to Electroporation and Electrofusion, ed by D.C. Chang et al, (Academic, San Diego, 1992)

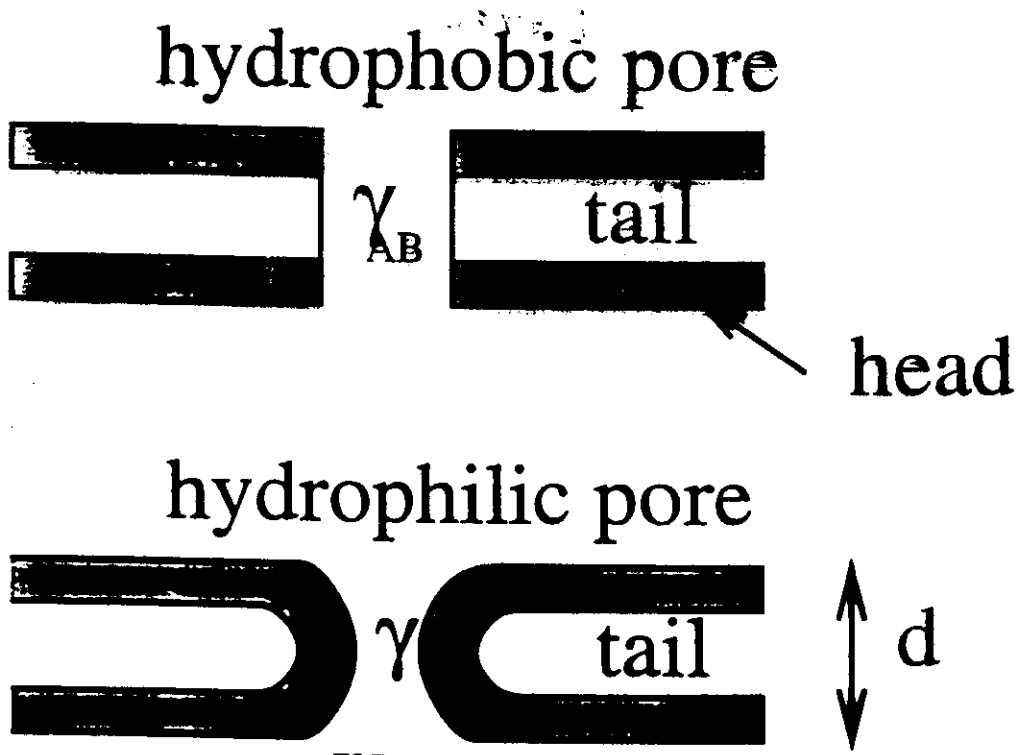

FIG. 18. Sketch of large hydrophobic and hydrophilic pores.

CHANGE ARCHITECTURE OF POLYMER SLIGHTLY ($f = 0.5$)

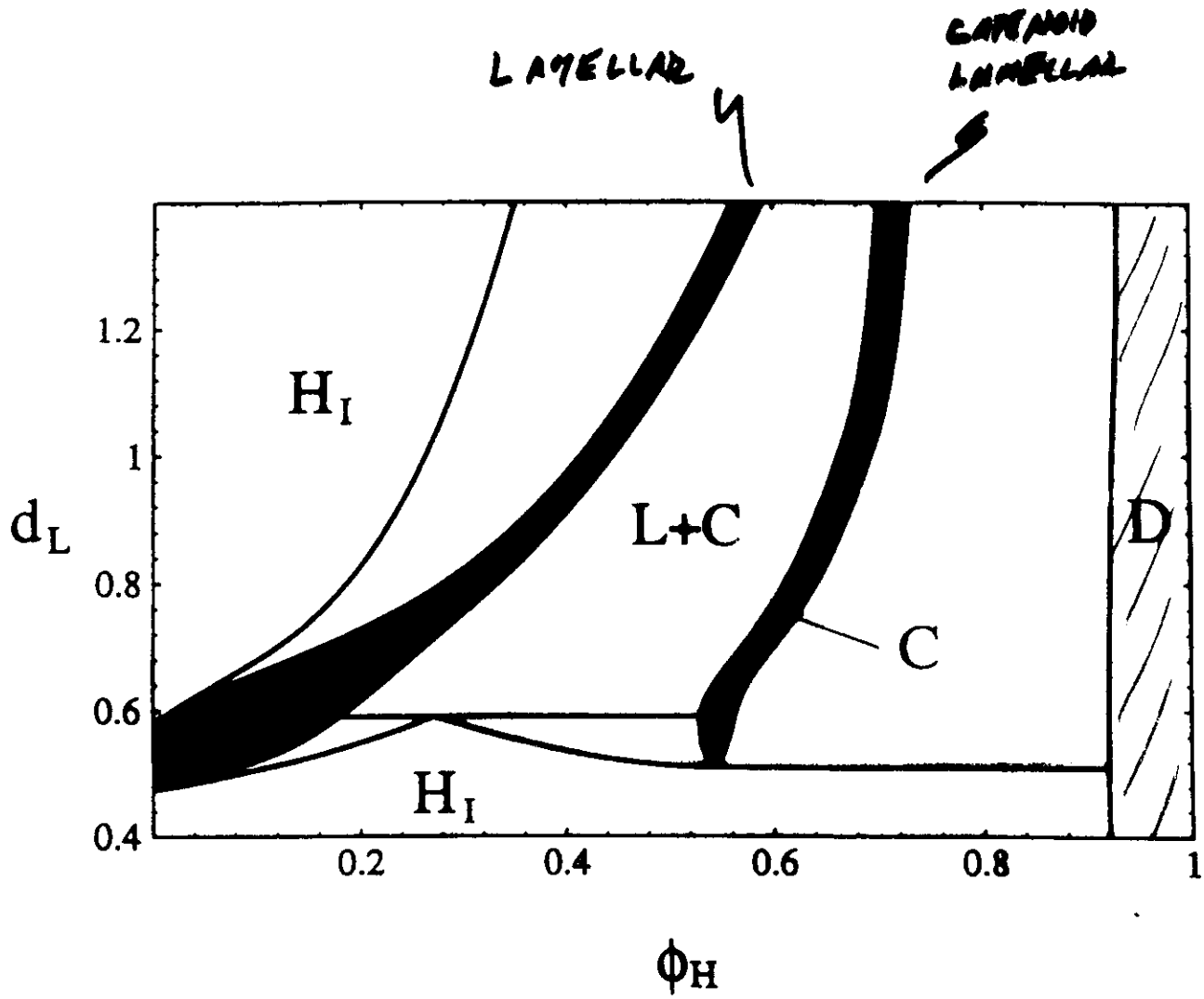

CLOSE PACKED ARRAY OF POLES IN EQUILIBRIUM

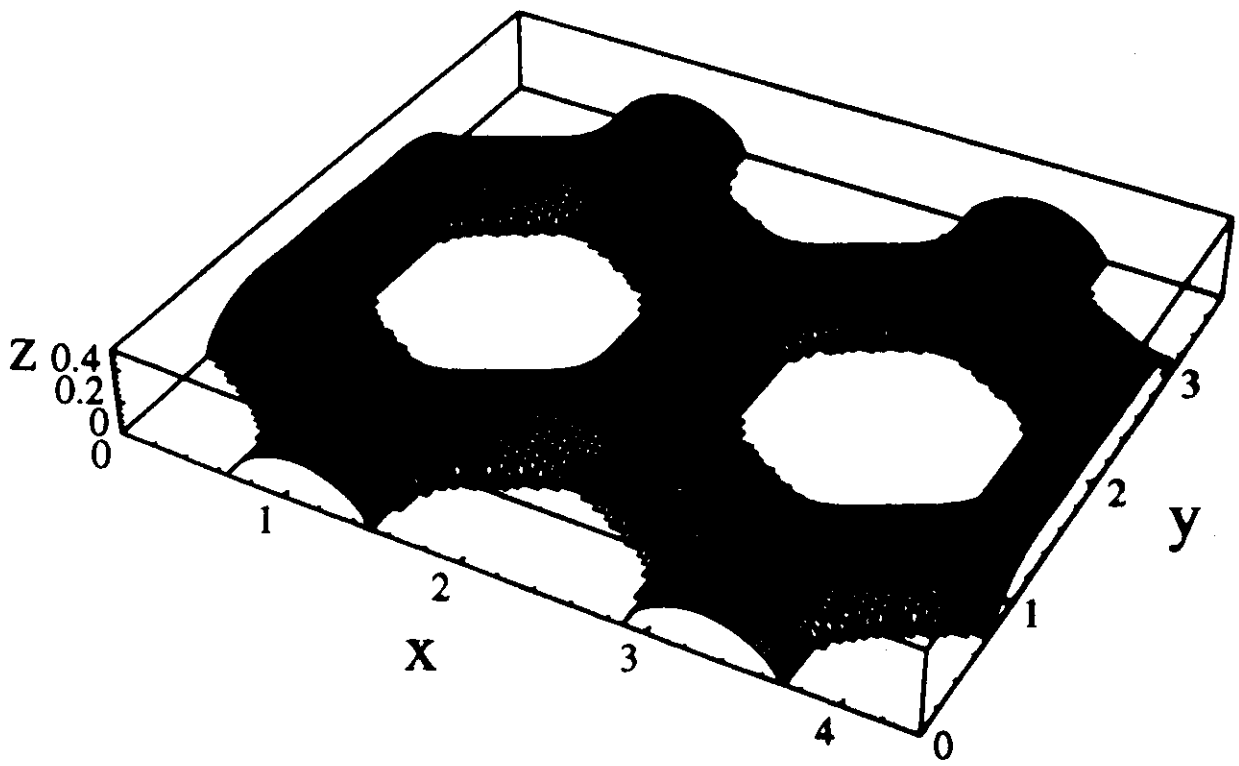

distances in units of the radius of gyration

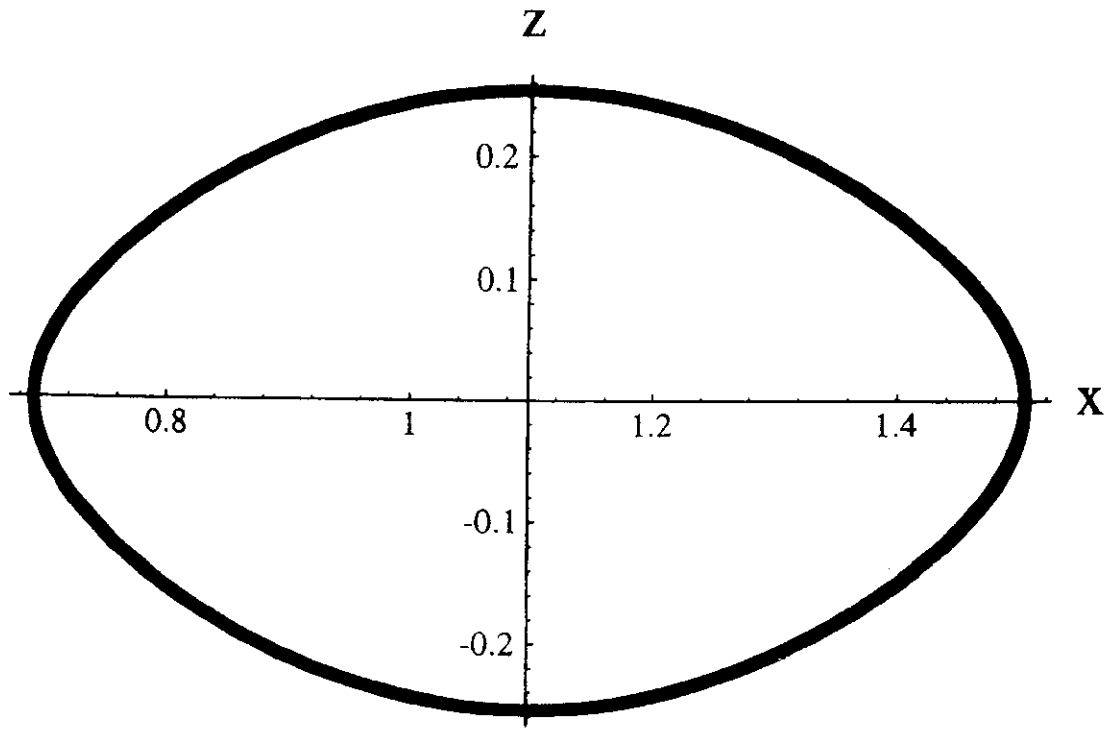
Z
0.2
0.1
0.8
1
1.2
1.4
X
-0.1
-0.2

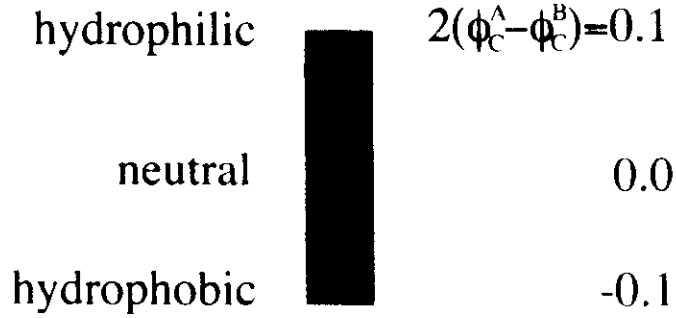
hydrophilic
$2(\phi_c^A-\phi_c^B)=0.1$
neutral
0.0
hydrophobic
-0.1

MONTE CARLO SIMULATION

Bond Fluctuation Model (Carmesin and Kremer, **Macromolecules 21**, 2819 (1988).)

Simple cubic lattice L× L× 2L, L=64 or 524,288 sites, lattice constant u

A monomer is represented by a cube which blocks eight corner sites

Adjacent monomers are connected via one of 108 bonds of length ranging from 2u to $\sqrt{10}$u

Chain lengths N_a=N_{AB}=32

Kuhn length a=3.05u

Radius of gyration R_g = 6.93u

Monomer volume fraction=0.5

$\chi N \approx 25$

MARCUS MUELLER

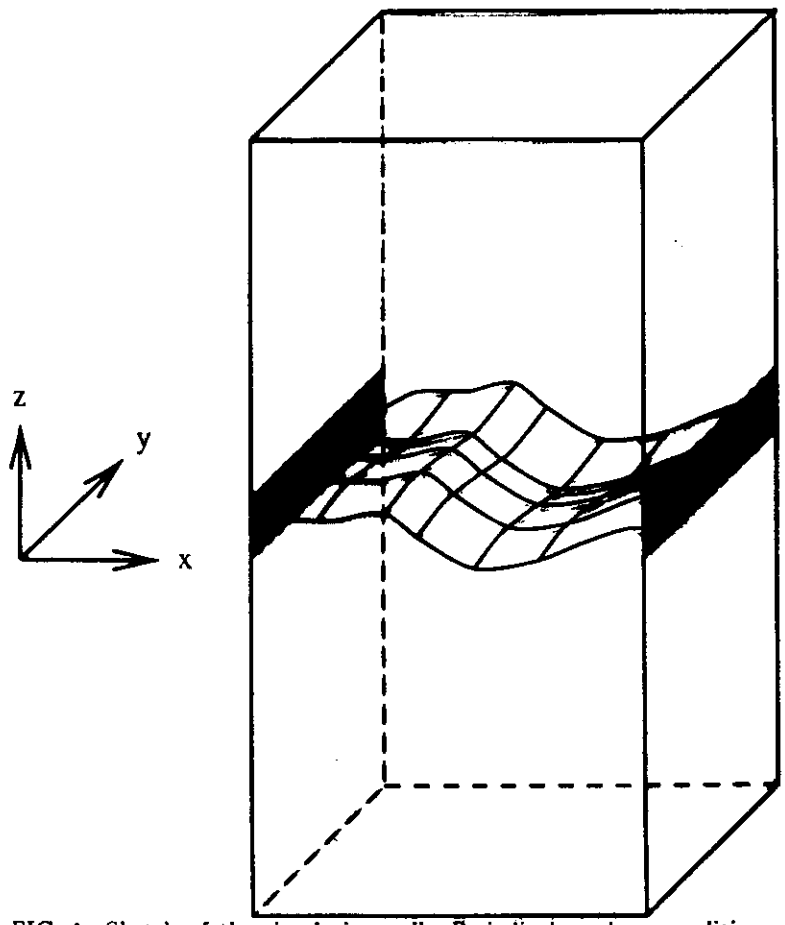

FIG. 1. Sketch of the simulation cell. Periodic boundary conditions are employed in the x and y direction, while there are impenetrable walls in z direction. The light shaded areas of the hard walls attract hydrophobic segments, whereas the dark shaded favor hydrophilic ones. A bilayer forms around $z = 64$ in the xy-plane.

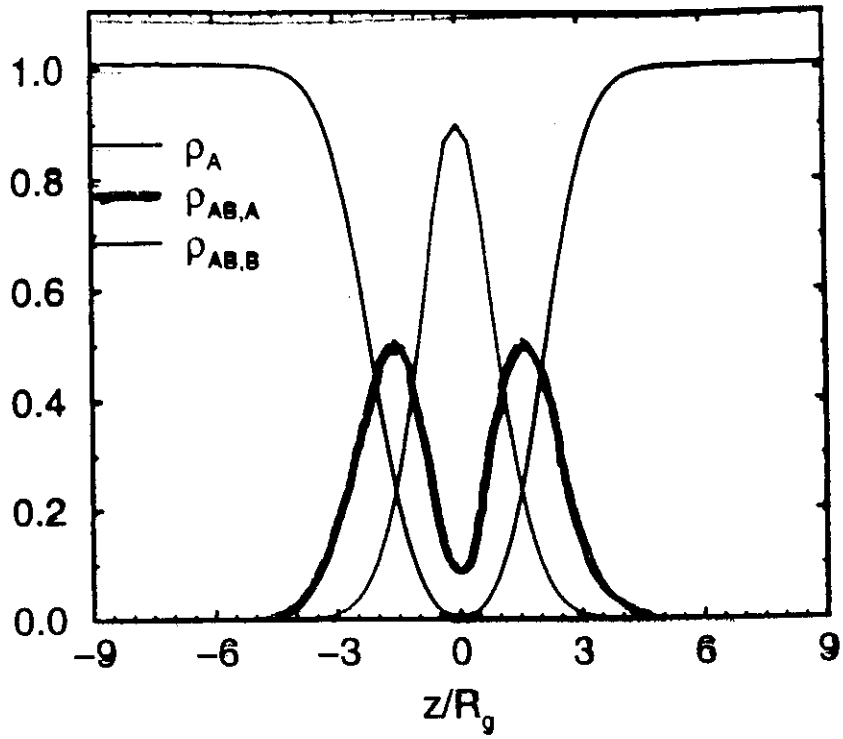

FIG. 4. Composition profile across a bilayer at $\epsilon = 0.15$ and $\Delta\mu = 4.5$. The solid line show of homopolymer, the dashed line corresponds to the head segment density of the amphiphil line to the tail segment density .

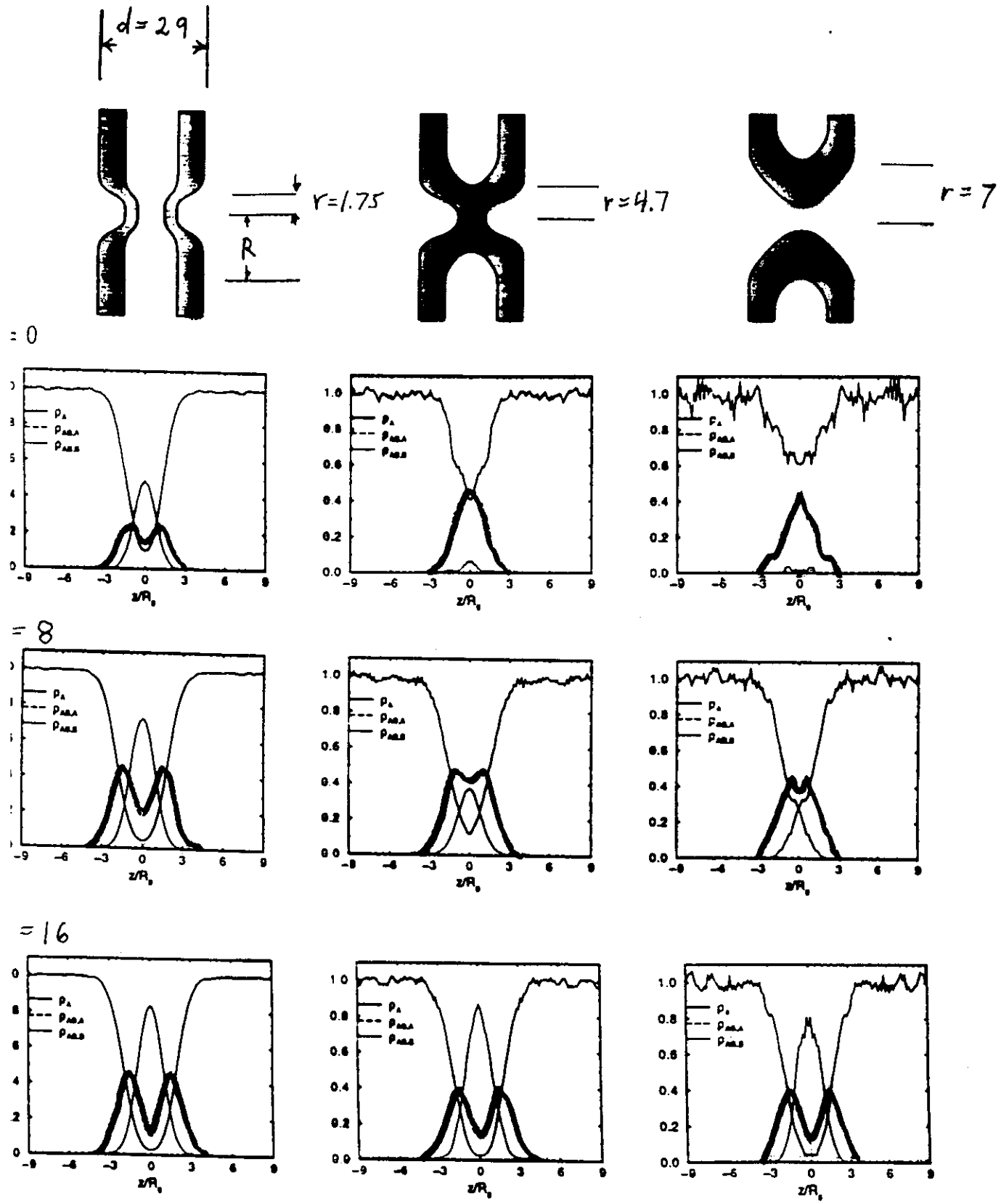

. 19. Composition profiles across a bilayer at distances $R = 0,$ 8, 16 from the center of the pore (from bottom) for three different pore sizes; $r \approx 1.75$ ($\mathcal{N} = 1$), $r \approx 4.7$ ($\mathcal{N} = 6, 7, 8$), and $r \approx 7.0$ ($\mathcal{N} = 15, 16, 17$) left to right). The upper row shows sketchs of the pores infered from the detailed composition profiles. The rger pores are hydrophobic.

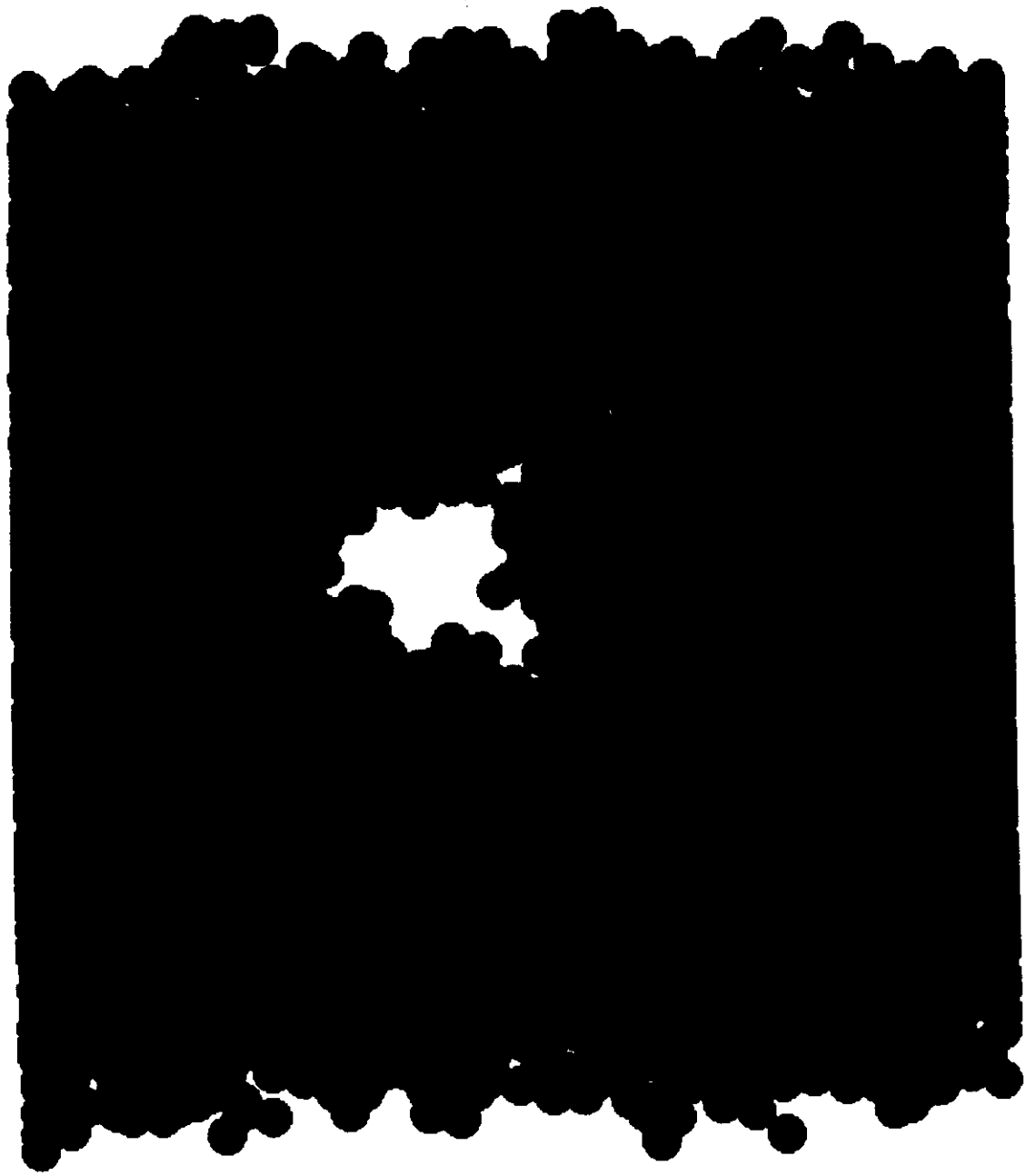

What is the free energy/unit, γ, area of this bilayer?

Obtain it from the fluctuation spectrum

of bilayer position $u(\mathbf{r})$

$$H = \frac{\gamma}{2} \int dx\, dy\, (\nabla u)^2$$

From equipartition

$$\frac{2}{L^2 < u_q^2 >} = \gamma q^2$$

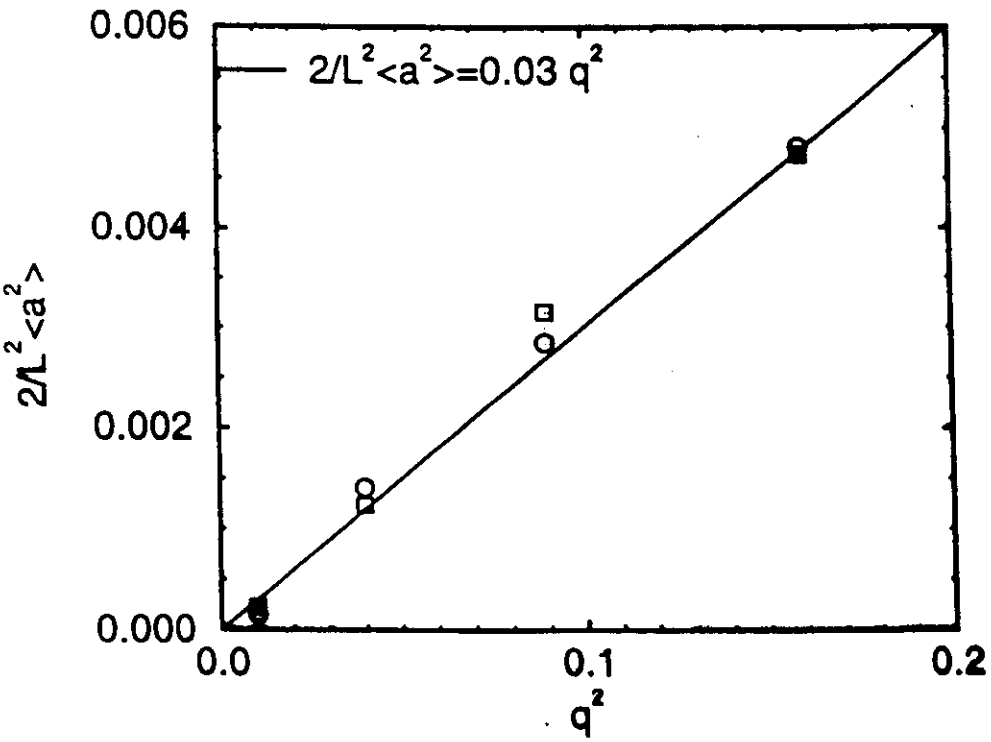

FIG. 8. Low wavevector regime of the bilayer undulation spectrum at $\epsilon = 0.15$ and $\Delta\mu =$ .5. Solid Line corresponds to a tension of $\gamma = 0.030(5)$.

$\gamma < 2\gamma_{AB} = 0.132$

What is the line tension of the pore?

Obtain it from the distribution of pore sizes, P(r)

$$\ln\ P(r) = -\delta f = -2\pi r\Gamma + \pi r^2\gamma + \text{constant}$$

Define

$$\Gamma = r\gamma - \frac{1}{2\pi}\frac{d}{dr}\ln P(r)$$

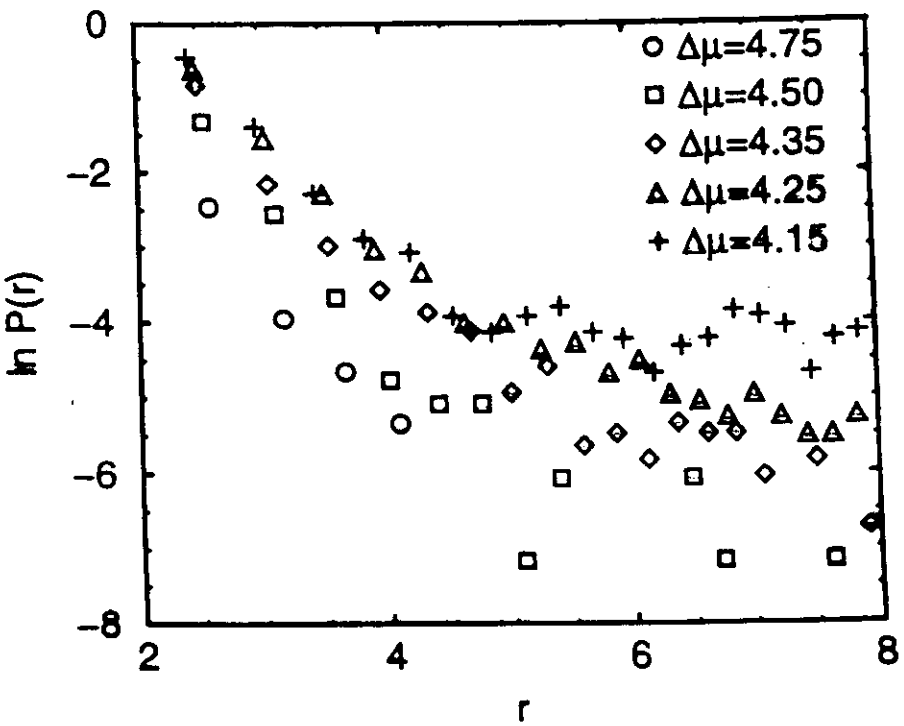

FIG. 15. Probability distribution of pore sizes at various chemical potentials. In the accessible range of pore sizes, no prefered pore size can be observed.

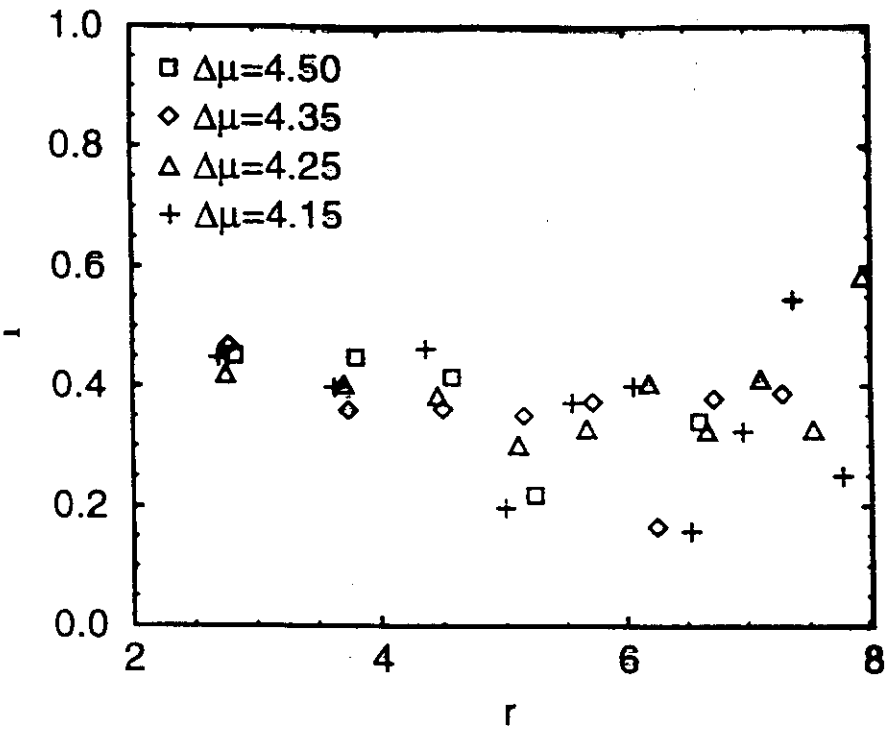

G. 17. Simulation results for the effective edge tension Γ for various chemical potentials. The edge tension rgely independent of the chemical potential of the amphiphile and of the size of the pore.

SUMMARY OF BILAYER PROPERTIES

Equate bilayer thickness to 30Å

1. γ_{AB} (oil/water tension) $\approx$ 27 erg/cm^2 (c.f. 50 erg/cm^2)
2. γ (membrane tension) $\approx$ 12 erg/cm^2 (c.f. 1 erg/cm^2)
3. area per tail $\approx$ 35Å^2 (good agreement)
4. surface compressibility modulus $\approx$ 83 erg/cm^2 (120 erg/cm^2 for phosphatidylcholine)
5. line tension $\Gamma \approx 1.710^{-6}$ erg/cm (correct order of magnitude)

Bilayers of Semi-Flexible Copolymer

Interactions

$$\chi \int d\mathbf{r} \hat{\Phi}_A(\mathbf{r}) \hat{\Phi}_B(\mathbf{r}) - \tau_Q \int d\mathbf{r} S^2(\mathbf{r})$$

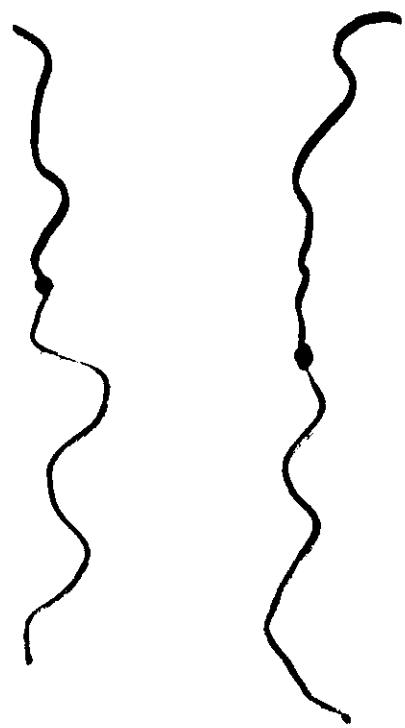

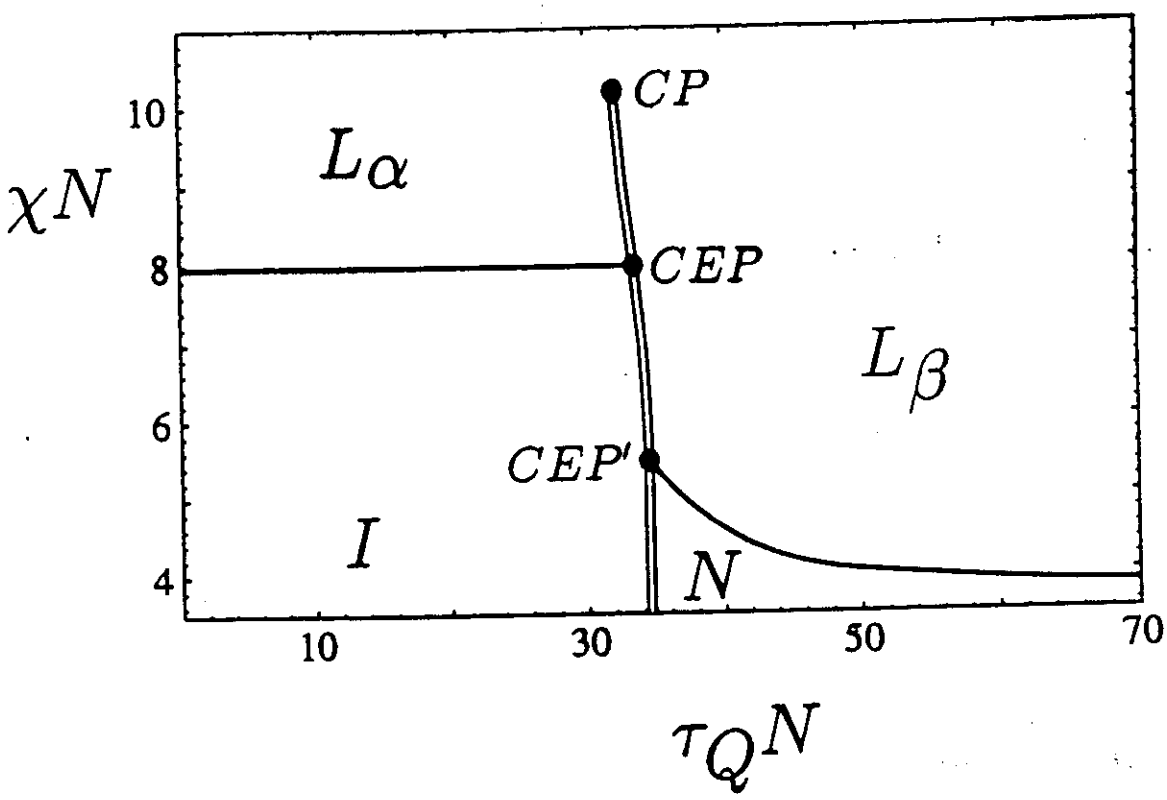

R. R. NETZ + M. S.

PRL JULY 1996

THANKS TO

ROLAND NETZ

MARCUS MUELLER

PHILIPP JANFAT

MICHAEL WORTH

FRANK JÜLICHER

NATO

HUMBOLDT STIFTUNG

NSF